https://doi.org/10.1093/plphys/kiae103 PLANT PHYSIOLOGY 2024: 00: 1–16

Plant Physiology®

Research Article

Plant iron status regulates ammonium-use efficiency through protein N-glycosylation

Guangjie Li[1,2,*] **Lin Zhang**[1] **Jinlin Wu**[2,3] **Zhaoyue Wang**[2,3] **Meng Wang**[2,3] **Herbert J. Kronzucker**[4] **Weiming Shi**[2,3,5,*]

1 State Key Laboratory of Nutrient Use and Management, Institute of Agricultural Resources and Environment, Shandong Academy of Agricultural Sciences, Jinan 250100, China
2 State Key Laboratory of Soil and Sustainable Agriculture, Institute of Soil Science, Chinese Academy of Sciences, Nanjing 210008, China
3 College of Advanced Agricultural Sciences, University of the Chinese Academy of Sciences, No. 19(A) Yuquan Road, Shijingshan District, Beijing 100049, China
4 School of BioSciences, The University of Melbourne, Parkville, VIC 3010, Australia
5 International Research Centre for Environmental Membrane Biology, Foshan University, Foshan 528000, China

*Author for correspondence: wmshi@issas.ac.cn (W.S.), ligjsaas@163.com (G.L.)
The author responsible for distribution of materials integral to the findings presented in this article in accordance with the policy described in the Instructions for Authors (https://academic.oup.com/plphys/pages/General-Instructions) is Weiming Shi (wmshi@issas.ac.cn).

Abstract

Improving nitrogen-use efficiency is an important path toward enhancing crop yield and alleviating the environmental impacts of fertilizer use. Ammonium (NH_4^+) is the energetically preferred inorganic N source for plants. The interaction of NH_4^+ with other nutrients is a chief determinant of ammonium-use efficiency (AUE) and of the tipping point toward ammonium toxicity, but these interactions have remained ill-defined. Here, we report that iron (Fe) accumulation is a critical factor determining AUE and have identified a substance that can enhance AUE by manipulating Fe availability. Fe accumulation under NH_4^+ nutrition induces NH_4^+ efflux in the root system, reducing both growth and AUE in Arabidopsis (*Arabidopsis thaliana*). Low external availability of Fe and a low plant Fe status substantially enhance protein N-glycosylation through a Vitamin C1-independent pathway, thereby reducing NH_4^+ efflux to increase AUE during the vegetative stage in *Arabidopsis* under elevated NH_4^+ supply. We confirm the validity of the iron–ammonium interaction in the important crop species lettuce (*Lactuca sativa*). We further show that dolomite can act as an effective substrate to subdue Fe accumulation under NH_4^+ nutrition by reducing the expression of *Low Phosphate Root 2* and acidification of the rhizosphere. Our findings present a strategy to improve AUE and reveal the underlying molecular–physiological mechanism.

Introduction

Ammonium (NH_4^+) and nitrate (NO_3^-) are the main sources of nitrogen (N) for most plants, and plants differ enormously in the extent to which they can thrive on either N source (Kronzucker et al. 1997, 2000, 2003). NO_3^- must be reduced to NH_4^+ before it can be incorporated into amino acids, proteins, and other macromolecules, a process that requires energy (Britto and Kronzucker 2005; Hachiya et al. 2007; Meier et al. 2020; Vidal et al. 2020), and thus, ammonium is considered the preferred nitrogen source in terms of energy costs, except in species that suffer ammonium toxicity already at relatively low concentrations—in the latter, elevated respiration rates and a negative energy balance are frequently observed (Britto et al. 2001). Increasing NH_4^+ use by plants has been suggested to be an important goal for agriculture as CO_2 levels rise in the world (Hachiya et al. 2021; Subbarao and Searchinger 2021). In farmland soil solutions, bulk NH_4^+ concentrations are normally in the micromolar range, but can fall into the of 2 to 20 mM range, and, in some cases, be as high as 40 mM following fertilizer application (Britto and Kronzucker 2002; Ma et al. 2016). However, typically only 30% to 50% of applied N fertilizer is taken up by crops, with the remainder being emitted into the atmosphere as ammonia (NH_3) (Coskun et al. 2017a, 2017b) or, following

Received January 08, 2024. Accepted January 25, 2024. Advance access publication February 24, 2024.

nitrification, lost as N-oxide gases or leached as nitrate into water systems where it causes eutrophication (Sun et al. 2015; Coskun et al. 2017a, 2017b; Min et al. 2021). Since the global food demand is continually rising, simply limiting N fertilizer inputs and sacrificing yield is clearly not feasible, especially not in most developing countries. Thus, determining how to enhance plant growth by increasing nitrogen-use efficiency (NUE), and its subset, ammonium-use efficiency (AUE), is an urgent challenge in agriculture.

Great progress has been made in approaches to optimize nitrate-use efficiency in various plant species, by targeting nitrate absorption, metabolism, and remobilization (Tsay et al. 1993; Huang et al. 2009; Xu et al. 2012; Hu et al. 2015; Fan et al. 2016; Ohkubo et al. 2017; Chen et al. 2020a; Liu et al. 2023a; Song et al. 2023). Previous attempts have also been made to improve AUE by increasing ammonium absorption and metabolism. However, some studies have shown that increasing ammonium transporter-mediated ammonium absorption can exacerbate ammonium toxicity (Hoque et al. 2006; Bao et al. 2015). Recent reports have further shown that excessive ammonium metabolism by plastidic glutamine synthetase (GS) can bring about ammonium toxicity (Hachiya et al. 2021; Xie et al. 2023). Low AUE is frequently associated with futile NH_4^+ cycling in roots, and larger NH_4^+ efflux in roots has been observed in low-NUE cultivars under high NH_4^+ (Chen et al. 2013, 2020b). Although the factors and/or mechanisms controlling NH_4^+ efflux from plant roots are still poorly understood, it has been suggested that protein N-glycosylation alteration is associated with NH_4^+ efflux regulation (Qin et al. 2008; Li et al. 2010, 2014, 2022; Di et al. 2021). Higher protein N-glycosylation is associated with reduced NH_4^+ efflux and protecting growth under elevated NH_4^+ (Qin et al. 2008; Tanaka et al. 2015; Li et al. 2022). GDP-mannose pyrophosphorylase (GMPase) has been reported to be involved in the regulation of plant growth under high NH_4^+ by regulating protein N-glycosylation. Mutation in *Vitamin C1* (*VTC1*) results in enhanced root NH_4^+ efflux, linking N-glycosylation of proteins functionally to root NH_4^+ fluxes (Qin et al. 2008; Barth et al. 2010; Li et al. 2010; Kempinski et al. 2011). All the previous studies suggest that, in addition to primary ammonium absorption and/or metabolism, there must be other factors limiting the improvement of AUE.

Nutrient interaction has been shown to be important for the presentation of ammonium toxicity symptoms in many plants (Kronzucker et al. 1999; Szczerba et al. 2008; Balkos et al. 2010; Britto et al. 2014; Xiao et al. 2022; Coleto et al. 2021, 2023). Intriguingly, NH_4^+ can decrease the tissue contents of most cations but increase the content of iron (Fe) (Britto and Kronzucker 2002; Roosta and Schjoerring 2007; Li et al. 2012, 2013). Recently, Liu et al. (2022a, 2023b) found that NH_4^+-regulated Low Phosphate Root 2 (LPR2)-mediated aberrant Fe accumulation impairs Arabidopsis (*Arabidopsis thaliana*) root growth. Meanwhile, Pyridoxine Biosynthesis 1.1 (PDX1.1)-dependent biosynthesis of vitamin B6 was shown to protect root elongation from Fe-accumulation stress under NH_4^+ conditions (Liu et al. 2022b). These reports suggest that Fe plays a role in the regulation of root elongation under NH_4^+ nutrition.

In this work, we show that Fe accumulation under NH_4^+ nutrition is indeed a critical factor in the regulation of root NH_4^+ efflux, AUE, and plant growth in both Arabidopsis and lettuce (*Lactuca sativa*). We further report that low external availability of Fe or low Fe status of the plant substantially enhance protein N-glycosylation through a VTC1-independent pathway, thereby reducing NH_4^+ efflux to increase AUE during the vegetative stage in Arabidopsis under high-NH_4^+ conditions. We identify dolomite as an effective substrate to control Fe accumulation under NH_4^+ nutrition by reducing ammonium-linked *LPR2* gene expression and rhizosphere acidification.

Results

Fe regulates Arabidopsis growth and AUE under high $NH4^+$ supply

Experiments were designed to examine the growth of Arabidopsis on media with different combinations of NH_4^+ and Fe. We found that when Arabidopsis was grown on normal growth medium (GM) containing a standard Fe concentration of 100 μM (Fe^{100}), Arabidopsis rosette size and dry weight (DW) of whole seedlings were only slightly increased in NH_4^+ medium compared to in the mock condition (Fig. 1, A and B). On medium containing 5 μM Fe (Fe^5), Arabidopsis growth was markedly different and was strongly promoted by NH_4^+ (Fig. 1, A and B; Supplementary Fig. S1A). Rosette size and DW of whole seedlings under $Fe^5 + NH_4^+$ were increased by ∼27% and ∼35%, respectively, compared to those of Col-0 seedlings grown on $Fe^{100} + NH_4^+$ (Fig. 1, A and B). Similar experiments were performed using equipotent $FeSO_4$ and/or $FeCl_3$–EDTA, and even with these different forms, Fe^{100} led to lower seedling growth than Fe^5 under NH_4^+ treatment (Supplementary Fig. S1B). However, low Fe status did not enhance plant growth in either the GM control (mock) or the equimolar-nitrate ($+NO_3^-$) conditions (Fig. 1, A and B).

We further examined whether AUE can be affected by Fe availability. The N usage index (UI), which is calculated by dividing seedling DW by seedling N content (Wada et al. 2015; Chen et al. 2020a), is suitable for estimating NUE (or AUE) at the vegetative stage (Good et al. 2004; Brauer and Shelp 2010). N content and N UI were highest in the $Fe^5 + NH_4^+$ seedlings (e.g. UI increased by ∼19% to 34%) compared to all other treatments (Fig. 1, C and D), indicating that low Fe status enhances plant vegetative growth and AUE under conditions of elevated NH_4^+. However, low Fe status did not enhance UI in the equimolar nitrate ($+NO_3^-$) treatments (Fig. 1, C and D). Furthermore, there was no difference in either GS or total plant carbon (C) between Fe^{100} and Fe^5 under different nitrogen conditions (Supplementary Fig. S2), suggesting that the enhancement in AUE is not because low Fe status affects ammonium metabolism and/or

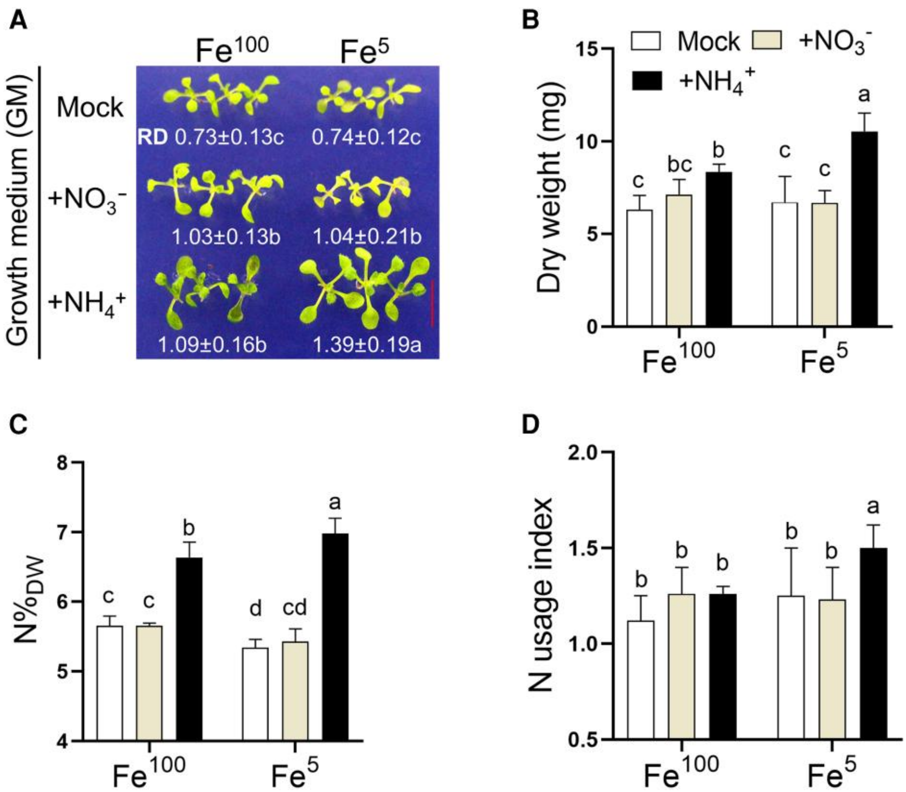

Figure 1. Fe regulates Arabidopsis growth and AUE under elevated NH_4^+. **A)** A representative photograph of shoots from the 10-d-old Col-0 grown on GM (mock) plus 5 mM NO_3^- (+NO_3^-) or 5 mM NH_4^+ (+NH_4^+) in Fe^5 (5 μM) and/or Fe^{100} (100 μM) medium. Bar = 1 cm. Rosette diameter (RD) is shown in the photograph. Values shown are the means ± SD ($n \geq 20$). **B)** Whole-seedling DW of 10-d-old Col-0 grown on mock, +NO_3^- and +NH_4^+ medium with Fe^5 and/or Fe^{100}. Twenty seedlings as a group, and values shown are the means ± SD of four group replicates. **C)** $N\%_{DW}$ of whole seedlings of 10-d-old Col-0 grown on mock, +NO_3^-, and +NH_4^+ medium with Fe^5 and/or Fe^{100}. N: nitrogen. Twenty seedlings as a group, and values shown are the means ± SD of four group replicates. **D)** UI by division of DW by $N\%_{DW}$. Values shown are the means ± SD of four group replicates. Different letters represent means that are statistically different at the 0.05 level (one-way ANOVA with Duncan post-hoc test).

carbon homeostasis under elevated NH_4^+. Moreover, there were no significant differences in NH_4^+ content or the contents of several other cations (e.g. K, Mg, Ca, Mn, Zn) between $Fe^5$and Fe^{100} under 5 mM NH_4^+ treatment (Supplementary Fig. S3), suggesting that the enhancement of seedling growth under NH_4^+ and low Fe is also not dependent on other elements. In order to test whether improved AUE under low Fe status and elevated NH_4^+ was caused by altered (higher) N-absorption activity in the roots, a $^{15}NO_3^-$ and $^{15}NH_4^+$ uptake experiment was performed. However, there was also no significant difference in ^{15}N uptake between Fe^5 and Fe^{100} under elevated NH_4^+ treatment (Supplementary Fig. S4). Taken together, these findings show that Fe accumulation presents a critical factor in regulating growth and AUE in Arabidopsis, and low Fe status improves AUE at the vegetative stage of Arabidopsis under elevated NH_4^+.

Low Fe status downregulates NH_4^+ efflux by upregulating protein N-glycosylation under high NH_4^+

Liu et al. (2022a) suggested that NH_4^+-mediated Fe(III) deposition in the tissues inhibits Arabidopsis root growth. Perls'Prussian Blue stain is a widely used acidic solution of potassium ferrocyanide, which reacts with ferric iron to form an insoluble blue precipitate (Green and Rogers 2004). To examine Fe accumulation under NH_4^+, we performed Perls Fe-staining (without 3,3′-diaminobenzidine intensification to avoid oversaturation). Under Fe^{100} conditions, the Perls staining intensity was much stronger in the NH_4^+-treated roots compared with the mock and/or Fe^5 conditions (Fig. 2A). The phenomenon was also observed by the ICP-MS method (Fig. 2B). Combining Fig. 1 and Fig. 2, A and B, we plotted tissue Fe level against seedling growth under +NH_4^+.

Previous studies have shown that increased NH_4^+ efflux in the roots is one of the key characteristics associated with root growth inhibition under high NH_4^+ (Britto et al. 2001; Li et al. 2010). As Fe negatively regulated plant growth under high NH_4^+, we asked whether the growth reduction was associated with elevated NH_4^+ efflux. We used the NMT technique to monitor the NH_4^+ net fluxes at the roots of Col-0 under both Fe^{100} and Fe^5. The roots of plants treated with Fe^{100} + NH_4^+ showed stronger NH_4^+ efflux than control plants (Fe^{100} − NH_4^+) (Fig. 2, C and D). Root NH_4^+ efflux was lower under the low Fe condition compared to that under the Fe^{100} + NH_4^+ condition (Fig. 2, C and D), and there was no difference in NH_4^+ efflux between Fe^5 + NH_4^+ and Fe^5 − NH_4^+ (Fig. 2, C and D).

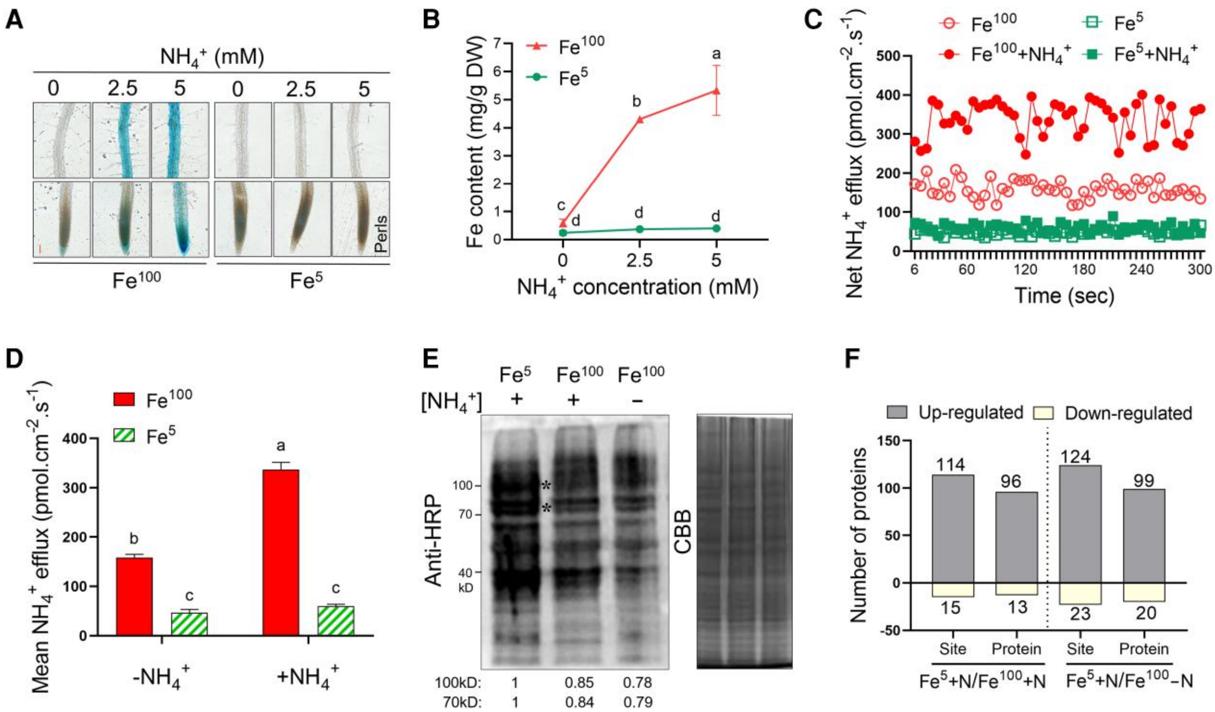

Figure 2. Low Fe status leads to downregulation of root NH_4^+ efflux by upregulating protein N-glycosylation under elevated NH_4^+. **A)** Root Fe staining (Perls staining) at different concentrations of NH_4^+ with Fe^5 (5 μM) or Fe^{100} (100 μM) medium. Bar = 200 μm. **B)** Fe content of Col-0 roots at different concentrations of NH_4^+ with Fe^5 or Fe^{100} medium. DW: dry weight. Values shown are the means ± SD of three replicates. **C, D)** Net NH_4^+ fluxes of Col-0 at the root tip transition zone, mean values of fluxes in (**C**) are shown in (**D**). $-NH_4^+$: 0 mM; $+NH_4^+$: 5 mM. Values are the means ± SD, $n = 6$ to 9 biological replicates. **E)** N-glycosylation of proteins in Col-0 roots 7 d post-germination at different concentrations of NH_4^+ and on Fe medium, evaluated using an anti-HRP reagent. Coomassie Brilliant Blue (CBB) staining of protein gels was used to control for protein loading. Asterisks (*) indicate different specific N-glycoprotein bands. The relative quantitative values of * are indicated at the bottom of the blots. **F)** Characteristics of differentially expressed N-glycoproteome in Col-0 roots 7 d post-germination. Protein: N-glycoproteins; site: N-glycosites from N-glycoproteins. $Fe^5 + N$: $Fe^5 + NH_4^+$; $Fe^{100} + N$: $Fe^{100} + NH_4^+$; $Fe^{100}-N$: $Fe^{100}-NH_4^+$. Different letters represent means that are statistically different at the 0.05 level (one-way ANOVA with Duncan post-hoc test).

Because higher protein N-glycosylation has been associated with reduced NH_4^+ efflux (Di et al. 2021; Li et al. 2022), we examined the extent of complex N-glycan formation using an anti-horseradish peroxidase (HRP) serum that directly binds to the oligomannose chains of N-glycoproteins (Strasser et al. 2004). N-glycoprotein of Col-0 under $Fe^5 + NH_4^+$ was higher than that under $Fe^{100} + NH_4^+$ (Fig. 2E). To further understand this result, a comparative N-glycoproteome assay, using indoTMTs with labeling, was performed. Gene Ontology (GO) analysis showed that the $Fe^5 + NH_4^+$ treatment resulted in substantial upregulation in N-glycosylation of proteins in Col-0 seedlings, compared with $Fe^{100} - NH_4^+$ and/or $Fe^{100} + NH_4^+$ (Fig. 2F; Supplementary Data Set 1). Collectively, these results indicate that low Fe status indeed downregulates root NH_4^+ efflux by upregulating protein N-glycosylation under high NH_4^+.

Low Fe status regulates NH_4^+ efflux and protein N-glycosylation through a VTC1-independent pathway

Previous studies have produced evidence indicating a critical role for VTC1 in controlling root NH_4^+ efflux in Arabidopsis under high NH_4^+ (Li et al. 2010; Di et al. 2021). Compared with Col-0, the *vtc1-1* mutant responded in a hypersensitive fashion to NH_4^+ (Fig. 3, A and B). The hypersensitive phenotype of *vtc1-1* in terms of seedling growth was also rescued by low Fe status (Fig. 3, A to D). For example, under the $Fe^{100} + NH_4^+$ treatment, Col-0 shoots were larger than those of *vtc1-1* mutants (Fig. 3C) and the DW of Col-0 seedlings was much higher than that of *vtc1-1* mutant seedings (Fig. 3D). By contrast, under $Fe^5 + NH_4^+$ conditions, the DW of the *vtc1-1* mutant was significantly higher than that of Col-0 under $Fe^{100} + NH_4^+$ (Fig. 3, C and D). However, under the $Fe^{100} + NH_4^+$ condition, Col-0 and *vtc1-1* roots showed comparable Fe levels in roots (Supplementary Fig. S5). This suggests that VTC1 acts downstream of the NH_4^+-induced Fe accumulation to regulate growth. We further determined whether low Fe status promotes UI in the NH_4^+-sensitivity mutant *vtc1-1* under high-NH_4^+ conditions. The UI of Col-0 was also higher than that of *vtc1-1* plants under the $+Fe^{100} + NH_4^+$ treatment (Fig. 3, E and F). In addition, low Fe levels led to a significant increase in both tissue N content and UI (increase by ~60%) in *vtc1-1* under high NH_4^+ (Fig. 3, E and F).

Measurements of net NH_4^+ fluxes in Col-0 and *vtc1-1* roots, assayed by NMT, revealed a significantly higher NH_4^+ efflux

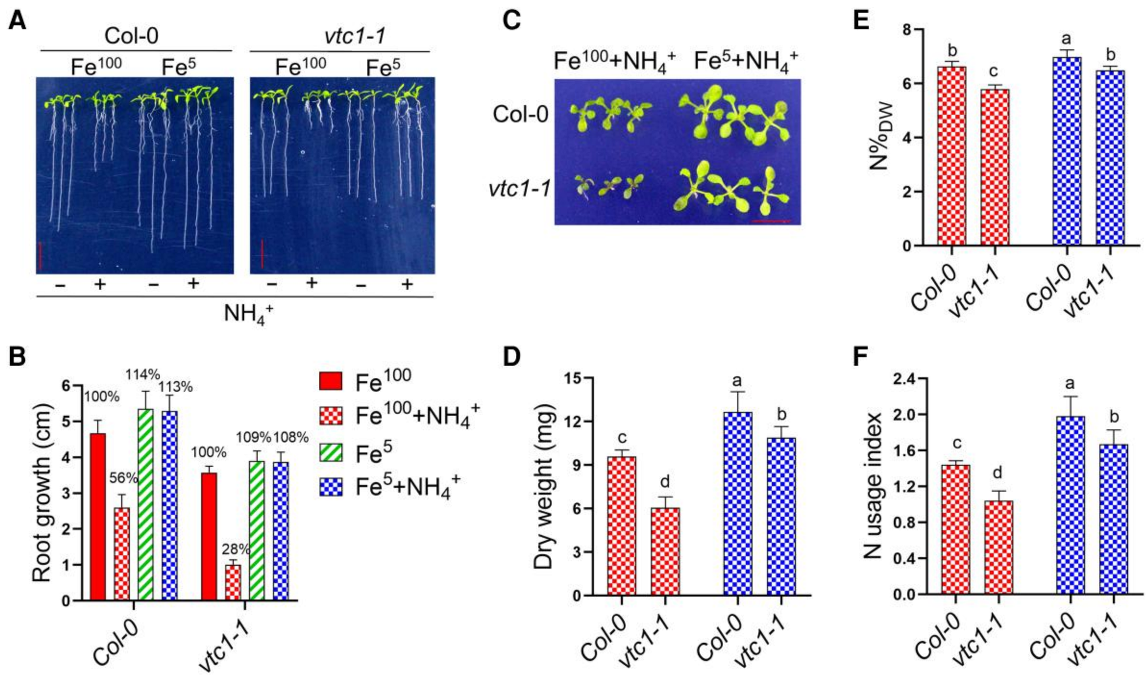

Figure 3. Low Fe status improves AUE in the *vtc1-1* mutant at the vegetative stage. **A, B)** Primary root growth of Col-0 and *vtc1-1* mutant. The medium was supplied with 0 ($-NH_4^+$) and/or 5 mM ($+NH_4^+$) NH_4^+ plus Fe^5 (5 μM) or Fe^{100} (100 μM), and root growth was evaluated 7 d post-germination. Bar = 1 cm. Values shown are the means ± SD ($n = 24$). **C)** A representative photograph of shoots from 10-d-old Col-0 and *vtc1-1* plants grown on 5 mM NH_4^+ medium with Fe^5 or Fe^{100}. Bar = 1 cm. **D)** Whole-seedling DW of 10-d-old Col-0 and *vtc1-1* plants grown on 5 mM NH_4^+ medium with Fe^5 or Fe^{100}. Twenty seedlings as a group, and values shown are the means ± SD of five group replicates. **E)** $N\%_{DW}$ of whole seedlings of 10-d-old Col-0 and *vtc1-1* plants grown on 5 mM NH_4^+ medium with Fe^5 or Fe^{100}. DW: dry weight; N: nitrogen. Twenty seedlings as a group, and values shown are the means ± SD of five group replicates. **F)** UI by division of DW by $N\%_{DW}$. Values shown are the means ± SD of five group replicates. Different letters represent means that are statistically different at the 0.05 level (one-way ANOVA with Duncan post-hoc test).

from the roots of *vtc1-1* than that from Col-0 roots when supplied with NH_4^+ under the Fe^{100} condition (Fig. 4A). NH_4^+ efflux under $Fe^5 + NH_4^+$ in Col-0 and *vtc1-1*, however, was lower than that under the $Fe^{100} + NH_4^+$ condition (Fig. 4A). Moreover, under the $Fe^5 + NH_4^+$ condition, Col-0 and *vtc1-1* plants showed comparable NH_4^+ efflux (Fig. 4A). VTC1 has been reported to be involved in regulating NH_4^+ efflux in Arabidopsis by regulating protein N-glycosylation (Qin et al. 2008; Li et al. 2010; Di et al. 2021). Compared with Col-0, the *vtc1-1* mutant contained less N-glycoprotein under the $Fe^{100} + NH_4^+$ treatment (Fig. 4B). Interestingly, low Fe treatment substantially enhanced the N-glycosylation level of the *vtc1-1* mutant under the $+NH_4^+$ treatment (Fig. 4B), suggesting that there was a VTC1-independent pathway at low Fe status that governs the upregulation of protein N-glycosylation under high NH_4^+. Furthermore, *NUDX9* (GDP-D-mannose pyrophosphohydrolase) expression in both Col-0 and *vtc1-1* roots was significantly reduced by low-Fe treatment following exposure to high NH_4^+ (Supplementary Fig. S6).

Increased Fe level induces VTC1 protein accumulation under high NH_4^+

We next determined whether, and, if so, how VTC1 is modulated by NH_4^+ and/or Fe. We monitored the level of endogenous VTC1 protein, using *35S:VTC1-GFP/vtc1-1* transformants, in response to different NH_4^+–Fe combination treatments. We found that the levels of VTC1-GFP protein dramatically rose following $Fe^{100} + NH_4^+$ treatment compared with in the absence of NH_4^+ (Fig. 4, C and D). However, in the presence of NH_4^+, Fe omission significantly reduced VTC1-GFP protein levels, suggesting that Fe but not NH_4^+ regulates VTC1 accumulation at the protein level (Fig. 4, C and D). To further analyze whether the increased Fe level induced VTC1 protein accumulation, we examined the response of VTC1-GFP to a high exogenous Fe level (Fe^{200}, 200 μM) in the absence of NH_4^+. When grown in the presence of a high Fe level without NH_4^+, there was significantly induced GFP abundance compared to that at low Fe (Fe^5) (Supplementary Fig. S7). Collectively, these results indicate that the regulation of VTC1 protein accumulation in NH_4^+-treated roots was Fe-dependent.

Dolomite attenuates NH_4^+ efflux by reducing Fe accumulation to promote Arabidopsis AUE

As AUE in plants is in part covered by NH_4^+ efflux from roots, we screened several compounds with the goal of identifying materials that might inhibit root NH_4^+ efflux. Selection of candidate compounds was based on reported mechanisms of ammonium and iron toxicity in plants, and included carbonates, antioxidants, and calcium compounds, and the screen

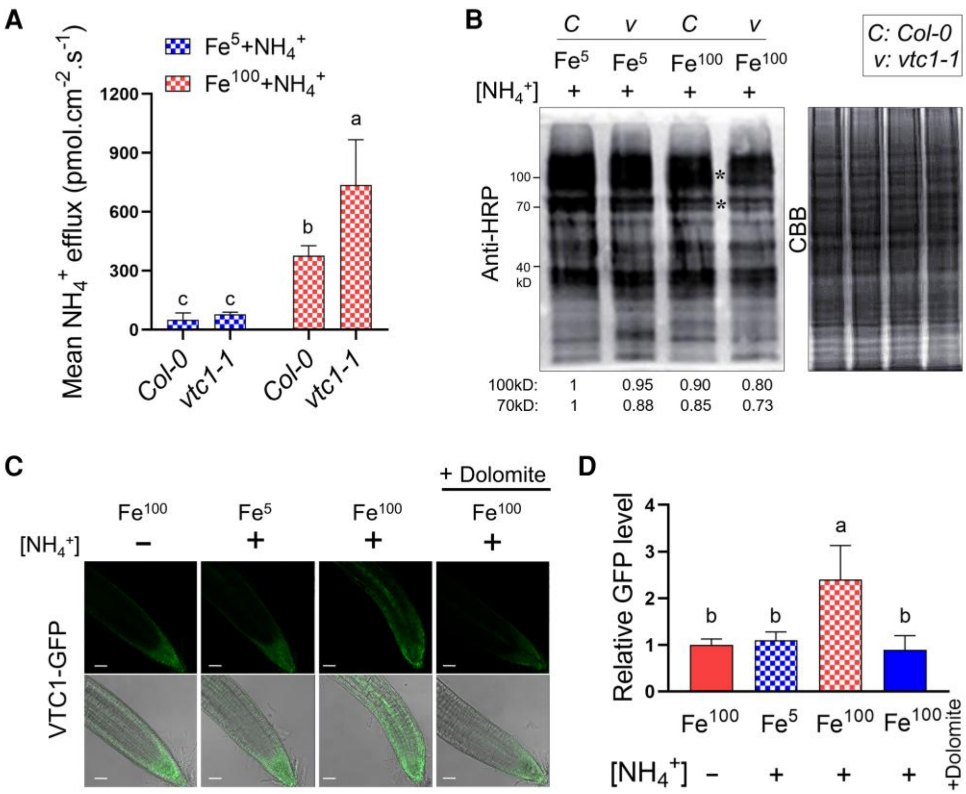

Figure 4. Effect of Fe on NH_4^+ efflux and protein N-glycosylation of the *vtc1-1* mutant under elevated NH_4^+. **A)** Mean values of NH_4^+ fluxes of Col-0 and *vtc1-1* at the root tip transition zone of plants grown on 5 mM NH_4^+ medium with Fe^5 (5 μM) or Fe^{100} (100 μM). Values are the means ± SD, $n = 9$ to 10 biological replicates. **B)** N-glycosylation of proteins in Col-0 and *vtc1-1* roots 7 d post-germination at different concentrations of Fe and on NH_4^+ medium, evaluated using an anti-HRP reagent. Coomassie Brilliant Blue (CBB) staining of protein gels was used to control for protein loading. Asterisks (*) indicate different specific N-glycoprotein bands. The relative quantitative values of * are indicated at the bottom of the blots. **C)** Localization of VTC1-GFP expression in transgenic *vtc1-1* plants. Green fluorescent protein (GFP) was observed 7 d post-germination under varying treatments. $-NH_4^+$: 0 mM, $+NH_4^+$: 5 mM; +dolomite: 5 g/L. Bar = 200 μm. **D)** The fluorescence of VTC1-GFP in (**A**). Fluorescence is expressed relative to that of $Fe^{100}-NH_4^+$. Values shown are the means ± SD of five replicates. Different letters represent means that are statistically different at the 0.05 level (one-way ANOVA with Duncan post-hoc test).

identified three compounds implicated in the reduction of NH_4^+ efflux. Dolomite emerged as the material associated with the largest reduction in NH_4^+ efflux, and was therefore used for further study (Supplementary Fig. S8). NH_4^+ efflux from both Col-0 and *vtc1-1* roots was significantly reduced by dolomite following exposure to high NH_4^+ (Fig. 5A). Moreover, under $+NH_4^+$ plus dolomite conditions, Col-0 and *vtc1-1* plants showed comparable NH_4^+ efflux (Fig. 5A). Dolomite application has been discussed previously as a potential management strategy for reducing plant iron toxicity (Suriyagoda et al. 2017). The response of NH_4^+ efflux under Fe overload suggested that dolomite could decrease NH_4^+-mediated Fe accumulation in Arabidopsis. This hypothesis was supported by the observation that exogenous application of dolomite had a substantially inhibitory effect on root Fe levels in both Col-0 and *vtc1-1* under high-NH_4^+ conditions (Fig. 5B). We also examined the level of VTC1-GFP in roots in response to dolomite under $Fe^{100} + NH_4^+$ and found that dolomite application led to a downregulation of VTC1-GFP abundance under the $Fe^{100} + NH_4^+$ treatment, further supporting that Fe accumulation induces VTC1 protein expression under high NH_4^+ (Fig. 4, C and D).

Experiments with varying dolomite concentrations (0, 1, and 5 g/L) were performed to investigate growth regulation by ammonium. As shown in Fig. 5, C and D, root growth under $Fe^{100} + NH_4^+$ was significantly enhanced by the application of varying dolomite concentrations in both Col-0 and *vtc1-1*. Consistently, rosette size and DW of whole seedlings following dolomite application were increased in Col-0 seedlings when grown on $Fe^{100} + NH_4^+$ (Fig. 5, E and F). Both tissue N content and UI with dolomite application was higher than under $Fe^{100} + NH_4^+$ treatments alone (Fig. 5G; Supplementary Fig. S9), indicating that dolomite application enhances Arabidopsis vegetative growth and AUE under high NH_4^+. However, dolomite ($CaMg(CO_3)_2$) did not enhance Col-0 growth in the absence of NH_4^+ (Supplementary Fig. S10). Roosta and Schjoerring (2008) found that the addition of calcium carbonate ($CaCO_3$) alleviated ammonium toxicity in cucumber (*Cucumis sativus*). Consistent with this, $CaCO_3$, rather than $CaCl_2$, promoted growth of Col-0 under high NH_4^+ (Supplementary Fig. S11). Collectively, the results show that dolomite can reduce NH_4^+-induced Fe accumulation to attenuate NH_4^+

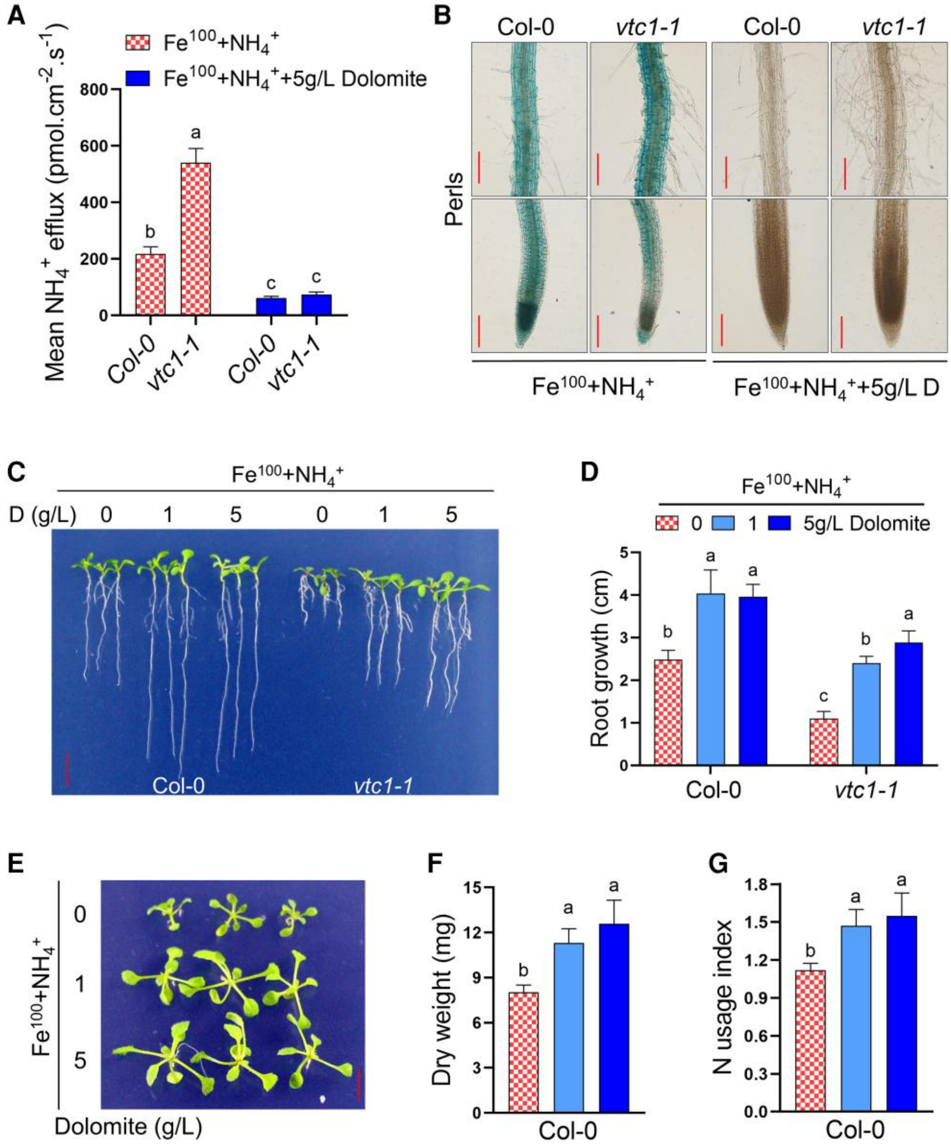

Figure 5. Dolomite reduces Fe accumulation to promote Arabidopsis growth and NUE under elevated NH_4^+. **A)** Mean values of NH_4^+ fluxes of Col-0 and *vtc1-1* at the root tip transition zone in plants grown on 5 mM NH_4^+ medium plus Fe^{100} (100 μM) with or without 5 g/L dolomite (D). Values are the means ± SD, $n = 9$ to 10 biological replicates. **B)** Appearance of root Fe staining (Perls staining) in Col-0 and *vtc1-1* mutant plants following treatment with 5 mM NH_4^+ medium plus Fe^{100} (100 μM) with or without 5 g/L dolomite (D) for 7 d. Bar = 200 μm. **C, D)** The effects of dolomite on root growth in Col-0 and *vtc1-1* mutant plants following treatment with Fe^{100} + NH_4^+ (100 μM Fe + 5 mM NH_4^+) plus 0, 1, or 5 g/L dolomite (D) for 7 day. Bar = 1 cm. Values shown are the means ± SD ($n = 12$). Different letters represent means that are statistically different at the 0.05 level in the same ecotype (one-way ANOVA with Duncan post-hoc test). **E)** Representative photograph of shoots from Col-0 grown on Fe^{100} + NH_4^+ plus 0, 1 or 5 g/L dolomite for 10 d. Bar = 1 cm. **F)** Whole-seedling DW of Col-0 grown on Fe^{100} + NH_4^+ plus 0, 1, or 5 g/L dolomite for 10 d. Twenty seedlings as a group, and values shown are the means ± SD of five group replicates. **G)** UI by division of DW (Fig. 5F) by $N\%_{DW}$ (Supplementary Fig. S6). Values shown are the means ± SD of five group replicates. Different letters represent means that are statistically different at the 0.05 level (one-way ANOVA with Duncan post-hoc test).

efflux and promote AUE in Arabidopsis at the vegetative stage.

Dolomite downregulates NH_4^+-dependent LPR2 expression

Since dolomite plays a critical role in regulating NH_4^+-mediated Fe accumulation, we further wondered how dolomite modulates Fe accumulation under NH_4^+ conditions. Medium acidification is a typical symptom of NH_4^+ treatment (Hachiya and Sakakibara 2017), and we first asked whether dolomite suppresses NH_4^+-mediated acidification of the rhizosphere (Britto and Kronzucker 2005). Significant rhizosphere acidification was detected in Col-0 grown in $+NH_4^+$ conditions, while rhizosphere acidification was weaker in the dolomite-supplied $+NH_4^+$ medium (Supplementary Fig. S12A).

Furthermore, a whole-transcriptome sequencing (RNA-seq) analysis of gene expression in both mock and dolomite-treated

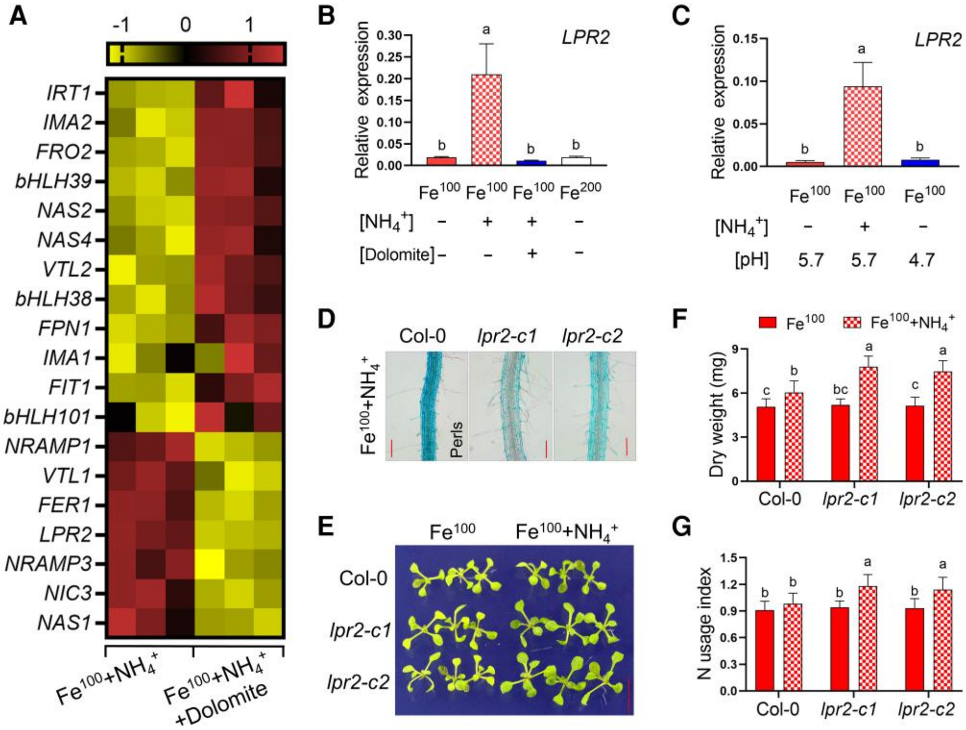

Figure 6. Dolomite treatment leads to downregulation of NH_4^+-dependent *LPR2* expression. **A)** Heatmap of dolomite-regulated Fe-response genes, created from RNA-seq data. Arabidopsis Col-0 seedlings grown in Fe^{100} + NH_4^+ medium with or without 5 g/L dolomite for 7 d, after which the roots were collected for RNA-seq analysis ($P < 0.01$). **B)** Effect of dolomite on gene expression of *LPR2* in 7-d-old Col-0 roots. $-NH_4^+$: 0 mM; $+NH_4^+$: 5 mM; Fe^{100}: 100 μM; Fe^{200}: 200 μM; +Dolomite: 5 g/L. Values shown are the means ± SD of five replicates. **C)** Effect of low pH on gene expression of *LPR2* in 7-d-old Col-0 roots. $-NH_4^+$: 0 mM; $+NH_4^+$: 5 mM; Fe^{100}: 100 μM. Values shown are the means ± SD of six replicates. **D)** Appearance of root Fe staining (Perls staining) of Col-0 and *LPR2* CRISPR/Cas9 editing plants following treatment with Fe^{100} + NH_4^+ (100 μM Fe + 5 mM NH_4^+) for 7 d. Bar = 200 μm. **E)** A representative photograph of shoots from the 10-d-old Col-0, *lpr2-c1*, and *lpr2-c2* grown on with or without 5 mM NH_4^+ medium plus 100 μM Fe (Fe^{100}). Bar = 1 cm. **F)** Whole-seedling DW of 10-d-old Col-0, *lpr2-c1*, and *lpr2-c2* grown with or without 5 mM NH_4^+ medium plus 100 μM Fe (Fe^{100}). Twenty seedlings as a group, and values shown are the means ± SD of five group replicates. **G)** UI of 10-d-old Col-0, *lpr2-c1*, and *lpr2-c2*. Values shown are the means ± SD of five group replicates. Different letters represent means that are statistically different at the 0.05 level (one-way ANOVA with Duncan post-hoc test).

Col-0 seedlings under Fe^{100} + NH_4^+ conditions (Supplementary Data Set 2) was performed. Of the genes encoding products involved in the Fe response, *LPR2*, which is known to encode a protein involved in NH_4^+-mediated root Fe accumulation (Liu et al. 2022a), was decreased by dolomite compared with mock under Fe^{100} + NH_4^+ (Fig. 6A; Supplementary Data Set 2). RT-qPCR analysis confirmed that *LPR2* was strongly induced by NH_4^+ but not in the presence of a high Fe level in roots (Fig. 6B), and dolomite could downregulate NH_4^+-dependent *LPR2* expression (Fig. 6B). We also examined whether low pH affects *LPR2* expression. However, RT-qPCR analysis showed that low pH treatment had no effect on *LPR2* expression in the absence of NH_4^+ (Fig. 6C), suggesting that dolomite downregulates *LPR2* expression not via pH regulation. Moreover, excess protons, produced as a by-product of ammonium assimilation, are pumped out by plasma-membrane (PM) H^+-ATPases and then induce acidification (Zhu et al. 2009; Zhang et al. 2018). Expression of *H^+-ATPase isoform 9* (*AHA9*) (Palmgren 2001) and *Proton Pump Interactor 2* (*Ppi2*), which encodes a protein that stimulates PM H^+-ATPase activity (Anzi et al. 2008), was distinctly decreased by dolomite treatment under NH_4^+ (Supplementary Data Set 2; Supplementary Fig. S12, B and C).

To validate the role of LPR2 in Fe-regulated AUE, we generated genome-edited alleles of *LPR2* by CRISPR/Cas9 editing (*lpr2-c1* and *lpr2-c2*) (Supplementary Fig. S13). Consistent with the previous report, the root Fe level of the *lpr2-c1* and *lpr2-c2* mutants was lower than that of Col-0 on a Fe^{100} + NH_4^+ medium (Fig. 6D). Phenotype analysis indicated that the *lpr2-c1* and *lpr2-c2* mutants had a growth advantage under Fe^{100} + NH_4^+ conditions (Fig. 6, E and F). The DW of the two mutants of *LPR2* was higher (increased by ~24% to 29%) than that of Col-0 plants, when they were directly germinated on a Fe^{100} + NH_4^+ medium (Fig. 6F). As shown in Fig. 6G, *lpr2-c1* and *lpr2-c2* plants showed a higher UI (increased by ~18% to 29%) than Col-0 plants under high NH_4^+. Collectively, these results indicate that dolomite downregulates NH_4^+-dependent *LPR2* expression, which is associated with NH_4^+-mediated Fe accumulation. Moreover, the response of the Arabidopsis *Iron-regulated transporter 1* (*IRT1*) and *Natural resistance-associated macrophage protein 1* (*NRAMP1*) mutations to ammonium was also assessed.

IRT1 is a major player in the regulation of plant iron homeostasis and facilitates high-affinity Fe uptake under Fe-deficient conditions in Arabidopsis (Vert et al. 2002). NRAMP1 also is a metal transporter and has been reported to regulate iron uptake in Arabidopsis (Castaings et al. 2016). As shown in Supplementary Fig. S14, however, Col-0, *irt1-2*, and *nramp1* knockout plants showed comparable root growth and Fe accumulation in roots under $Fe^{100} + NH_4^+$ conditions.

Fe regulates growth and AUE in lettuce under high NH_4^+

We have shown that low iron status successfully improves Arabidopsis growth and UI at the vegetative stage. To establish whether applying the same strategy might have a similar effect in other, more commercially important, plants, we also examined the effects of low Fe on lettuce (*L. sativa*), which is a widely consumed vegetable, and we analyzed growth and AUE under high NH_4^+. Consistently, plant size and DW under 10 μM Fe (Fe^{10}) were significantly larger than those of seedlings when grown on 100 (Fe^{100}) or 200 μM (Fe^{200}) Fe and NH_4^+ (Fig. 7, A and C). Meanwhile, Fe^{100} or Fe^{200} plus dolomite-treatment could increase DW by ∼41% and ∼130%, respectively, compared to mock condition (Fig. 7, A and C). An increasing Fe level was obtained under $Fe^{100} + NH_4^+$ conditions (Fig. 7B), but a lower Fe level was observed in the Fe^{10} and/or dolomite treatment roots under NH_4^+ condition (Fig. 7B). Furthermore, low-Fe- and/or dolomite-treated lettuce plants showed a higher $N\%_{DW}$ and UI under high NH_4^+ (Fig. 7, C and D). We further analyzed the effects of low iron status on lettuce plant yield and NUE. The lettuce plants were grown on GM plus 5 mM NO_3^- or 5 mM NH_4^+ for 30 d. The Fe^{10}-treated plants exhibited a larger size under the NH_4^+ condition than under the NO_3^- condition (Fig. 7E). More importantly, the yield per plant was highest under the $Fe^{10} + NH_4^+$ condition (Fig. 7F). Moreover, the NUE (as yield/supplied N) was also highest under the $Fe^{10} + NH_4^+$ condition (Fig. 7G). However, under equimolar $+NO_3^-$ treatment, there was no difference in lettuce growth or NUE between the Fe^{100} and Fe^{10} conditions (Fig. 7, F and G).

Discussion

Improving crop NUE is a key component in the quest to enhance yield while minimizing the environmental problems associated with N runoff, leaching, and outgassing losses from agricultural fields (Coskun et al. 2017a, 2017b). Many approaches and strategies have been taken to improve NUE for nitrate (NO_3^-) in various plant species (Chen et al. 2020a; Vidal et al. 2020; Wu et al. 2020; Liu et al. 2021). AUE has been studied less although, energetically, NH_4^+ is the preferred inorganic N source (Britto and Kronzucker 2005) and forecast to increase in importance for C_3 species in future environments of elevated CO_2 (Rubio-Asensio and Bloom 2017; Hachiya et al. 2021). It is still largely unknown what factors, including those brought about by various nutrient interactions, limit the improvement of AUE (Chen et al. 2013; Esteban et al. 2016; Hachiya et al. 2021; Liu and Xu 2023). Here, we found that Fe accumulation under ammonium nutrition is a crucial factor limiting AUE and have identified a substance that can effectively enhance AUE by manipulating Fe availability. Low external availability of Fe and/or Fe nutritional status of the plant substantially enhanced the growth, N content, and UI during the vegetative stage in Arabidopsis under elevated NH_4^+. When Fe was sufficient, there was no difference in the UI of Col-0 between the NH_4^+ addition and NH_4^+-free control condition (between $Fe^{100} + NH_4^+$ and $Fe^{100} - NH_4^+$), however, the UI was increased about 19% to 34% by lowering the level of external Fe under $+NH_4^+$ conditions compared to other treatment (Fig. 1D). Furthermore, dolomite-treated Col-0 plants with low Fe status under NH_4^+ nutrition displayed a ∼38% increase in the UI compared to mock plants in response to $Fe^{100} + NH_4^+$ (Fig. 5, E and G). Meanwhile, Arabidopsis *LPR2* mutants accumulated less Fe in tissue in response to NH_4^+, while displaying superior growth and UI compared to Col-0 (Fig. 6, D, F and G). Even the known ammonium-hypersensitive Arabidopsis mutant *vtc1-1* was still able to increase its UI by ∼60% at low Fe under high NH_4^+ (Fig. 3F). Furthermore, low external Fe and/or dolomite treatment increased biomass and AUE in *L. sativa*, a widely grown leafy vegetable, under elevated NH_4^+ (Fig. 7, B and D). It is important to note that the growth-promoting effects brought about by lowering iron status under ammonium nutrition cannot be achieved by removing iron completely, i.e. iron deficiency must be prevented (Supplementary Fig. S1A). Interestingly, low Fe status was not involved in improving the Arabidopsis UI for nitrate in our study (Fig. 1), suggesting a specific role of Fe in regulating AUE rather than NUE more generally. This conclusion was further supported by our experiments carried out in lettuce (Fig. 7, F and G).

Our work links plant Fe status and resultant performance differences on NH_4^+ media to protein N-glycosylation and root NH_4^+ efflux in agreement with earlier studies on mechanisms of alleviation from ammonium toxicity, both emerge as major factors governing AUE and growth when Fe status is manipulated (e.g. Figs. 2 and 4). Elevated NH_4^+ efflux in roots is a well-established mechanism linked to the development of ammonium toxicity and, therefore, plant growth (Britto et al. 2001; Kronzucker et al. 2001, 2003; Chen et al. 2013, 2020b). The data presented here indicate that root NH_4^+ efflux under ammonium is dependent on Fe status, and that, specifically, low Fe status can prevent the elevation of that efflux in Arabidopsis in response to NH_4^+ (Fig. 2, C and D). Our work shows that NH_4^+ levels in Arabidopsis roots are not different between Fe^5 and Fe^{100} (Supplementary Fig. S3), although Fe^{100}-treated roots display larger NH_4^+ efflux (Fig. 2, C and D), indicating that the changes in NH_4^+ efflux are not directly linked to NH_4^+ levels in roots (Di et al. 2021). Protein N-glycosylation has, as well, been previously successfully linked to the control of NH_4^+ efflux in roots and to protecting plant growth under high NH_4^+ (Li et al. 2010, 2022; Tanaka et al. 2015). We found here that ammonium-induced Fe accumulation can provide protection

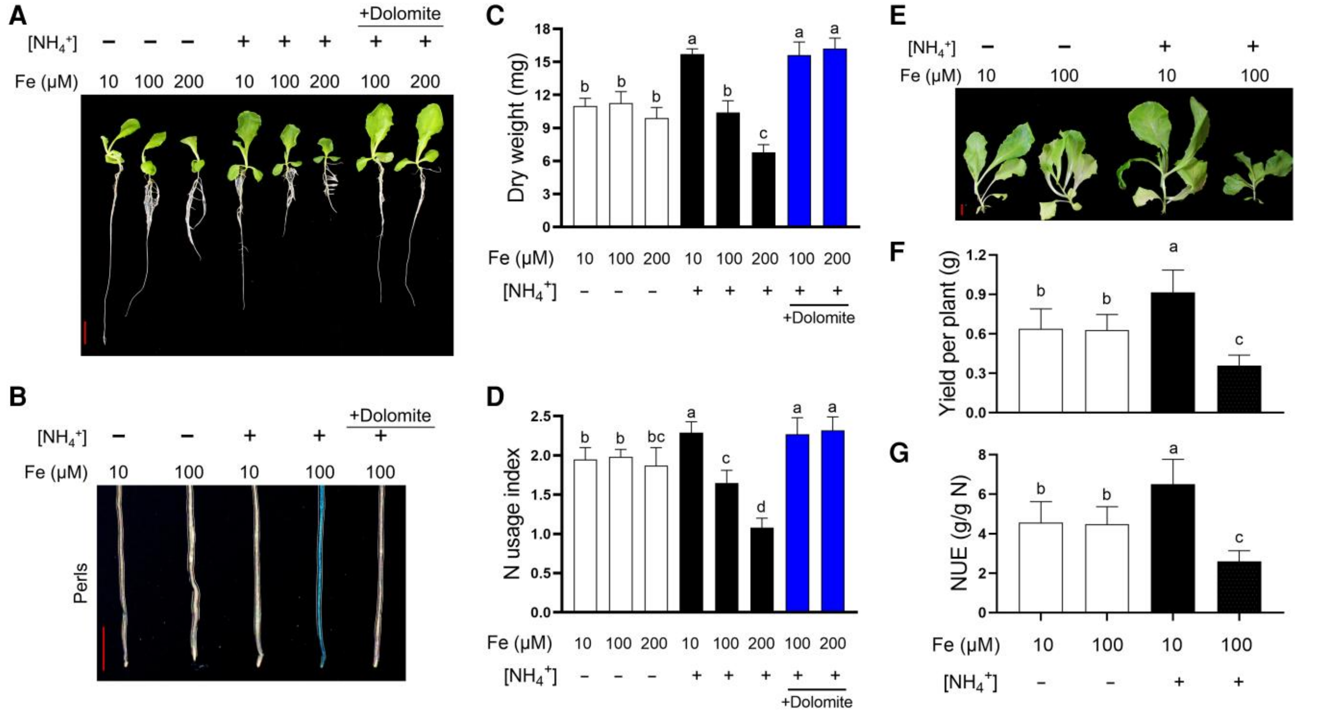

Figure 7. Low iron status promotes plant growth, yield, and AUE in lettuce. **A)** Representative photograph of lettuce from the 10-d-old seedlings under varying treatments. $-NH_4^+$: GM plus 5 mM NO_3^-; $+NH_4^+$: GM plus 5 mM NH_4^+; +Dolomite: 5 g/L. Bar = 1 cm. **B)** Lettuce root Fe staining (Perls staining) from 10-d-old seedlings under varying treatments. Bar = 1 cm. **C)** Whole-seedling DW of lettuce from 10-d-old seedlings under varying treatments. Three seedlings as a group, and values shown are the means ± SD of four group replicates. **D)** UI by division of DW by $N\%_{DW}$. Values shown are the means ± SD of four group replicates. **E)** Lettuce growth under Fe^{10} and Fe^{100} treatment and NO_3^- versus NH_4^+ conditions. Lettuce seedlings were grown on media for 30 d, and a representative photograph of shoots is displayed. Bar = 1 cm. **F)** Yield per plant. **G)** NUE of lettuce seedlings. Lettuce seedlings were grown on media for 30 d, and the yield (fresh weight of shoots) and NUE (yield/supplied nitrogen (N)) were analyzed. Data are presented as the means ± SD ($n = 8$ to 10). Different letters represent means that are statistically different at the 0.05 level (one-way ANOVA with Duncan post-hoc test).

by inducing N-glycosylation mediated via VTC1 (Figs. 2, E and F and 4, A and B), thereby partially inhibiting NH_4^+ efflux. Previous studies have shown that NH_4^+ can induce the accumulation of VTC1 protein (Zhang et al. 2021), and we here show that this induction depends on an increase in plant Fe levels (Fig. 4, C and D; Supplementary Fig. S7). Interestingly, under NH_4^+ treatment, low iron status can effectively enhance the protein N-glycosylation level in Col-0 Arabidopsis, and similar results are also seen in the *vtc1-1* mutant (Fig. 4B), suggesting that low iron status promotes N-glycosylation levels through pathways independent of *VTC1*. One possible explanation for how low Fe enhances *vtc1-1* N-glycosylation may relate to decreasing *NUDX9* expression under elevated NH_4^+ (Supplementary Fig. S6). Previous studies have demonstrated that increased GDP-D-mannose pyrophosphohydrolase (*NUDX9*) gene expression and activity could reduce GDP-mannose levels in roots, which subsequently repressed protein N-glycosylation in ammonium-treated roots in Arabidopsis (Tanaka et al. 2015; Di et al. 2021). However, the underlying molecular mechanisms will require further exploration.

Previous genetic studies demonstrated that Arabidopsis mutations in *VTC1* (Li et al. 2010), *NUDX9*, and *WRKY46* (Tanaka et al. 2015; Di et al. 2021) all lead to alterations in root NH_4^+ efflux. However, no compounds and/or pharmacological methods to reduce NH_4^+ efflux have emerged. Here, we report that dolomite can significantly reduce excess Fe accumulation under NH_4^+ nutrition and facilitate a reduction in NH_4^+ efflux in Arabidopsis roots (Fig. 5, A and B). Dolomite has previously been reported to modulate Fe toxicity in plants (Suriyagoda et al. 2017), and here we show its utility, and the linked mechanisms, for enhancing AUE in Arabidopsis. Liu et al. (2022b) have linked the well-established increase in proton secretion from roots and consequent medium acidification that take place during ammonium uptake (Britto and Kronzucker 2005) with increases in Fe solubilization in the rhizosphere along the Arabidopsis root. Under ammonium treatment, raising the pH of the medium or preventing rhizosphere acidification have been widely reported to be beneficial for alleviating ammonium toxicity and promoting plant growth (Britto and Kronzucker 2002; Kempinski et al. 2011; Hachiya et al. 2021; Liu et al. 2022b; Xiao et al. 2022). These previous, and our own, results suggest that dolomite application increases the pH of the root medium and prevents rhizosphere acidification (Suriyagoda et al. 2017; Supplementary Fig. S12A). Dolomite decreased *AHA9* and *Ppi2* expression, which may have led to the regulation of ammonium-mediated acidification (Supplementary Fig. S12, B and C), but further investigation is

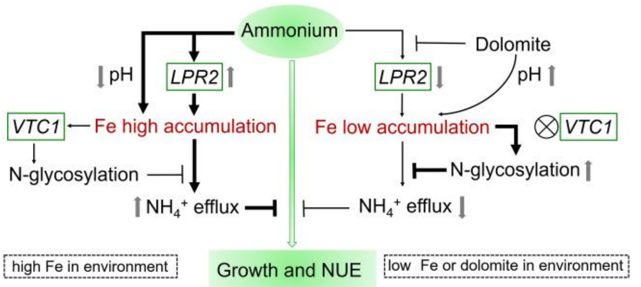

Figure 8. Schematic model of the mechanism of Arabidopsis growth and AUE regulation by Fe under elevated NH_4^+. Under a high iron (Fe) environment (left panel), ammonium-induced *LPR2* gene expression and rhizosphere acidification promote high tissue Fe accumulation. NH_4^+-mediated Fe accumulation restricts NH_4^+ efflux and its attenuation of growth and AUE in Arabidopsis. In comparison with a high-ammonium/high-Fe environment, a low Fe status enhances protein N-glycosylation via a *VTC1*-independent pathway to contribute to a reduction in root NH_4^+ efflux and consequent increase in AUE and plant growth (right panel). Dolomite application can reduce the Fe status of Arabidopsis seedlings under ammonium nutrition by inhibiting *LPR2* gene expression and rhizosphere acidification. The width of the black arrows and bars represents the physiological processes becoming stronger or weaker. The direction of the gray arrows represents the physiological processes and gene expression becoming up or down.

warranted. In addition, dolomite can impact the expression of genes related to the Fe response in Arabidopsis under Fe^{100} + NH_4^+ conditions (Fig. 6A). IRT1 facilitates high-affinity Fe uptake under Fe-deficient conditions (<1 μM) (Castaings et al. 2016). Consistent with this, the *irt1-2* mutant shows similar Fe levels and root growth to *Col-0* under abundant iron (100 μM) and +NH_4^+ conditions (Supplementary Fig. S14). Alternatively, recent studies showed that LPR2 controls iron translocation in Arabidopsis (Xu et al. 2022; Zhu et al. 2022). Dolomite reduces *LPR2* expression, while lowering LPR2 levels, and, thereby, helps reduce tissue Fe accumulation under ammonium nutrition (Liu et al. 2022a; Fig. 6B). Acidification of the medium did not induce *LPR2* expression in Arabidopsis in our study (Fig. 6C), suggesting that there are other ammonium- and/or dolomite-regulated *LPR2* expression responses that are independent of the acidification pathway, which deserves further study. $CaCO_3$ has also been demonstrated to be capable of alleviating ammonium toxicity (Roosta and Schjoerring 2008; Supplementary Fig. S11); mechanistically, carbon from carbonates, in the form of bicarbonate at cellular pH, can serve as a substrate for PEP carboxylase (Britto and Kronzucker 2005; Roosta and Schjoerring 2008; Balkos et al. 2010), stimulating NH_4^+ metabolism and drawing down free, potentially toxic, NH_4^+; this is then, in turn, linked to reductions in NH_4^+ efflux (Supplementary Fig. S8). Taken together, previous (Britto et al. 2001; Qin et al. 2008; Chen et al. 2013; Liu et al. 2022a, 2022b, 2023b) and present results lead us to propose a model for Fe-regulated growth and AUE in Arabidopsis under elevated NH_4^+ (Fig. 8). In a high-Fe environment, ammonium-induced *LPR2* gene expression and rhizosphere acidification promote high tissue Fe accumulation. NH_4^+-mediated Fe accumulation is then a crucial factor promoting NH_4^+ efflux in roots to attenuate growth and AUE. In comparison with conditions of high ammonium and high Fe, a low Fe status enhances protein N-glycosylation via a *VTC1* independent pathway to contribute to the reduction in NH_4^+ efflux and, thus, increase AUE and growth. Dolomite application can reduce Fe accumulation in Arabidopsis seedlings under ammonium nutrition by inhibiting *LPR2* gene expression and rhizosphere acidification. We believe that the unraveling of this mechanistic connection between plant Fe status and AUE brings us closer to an understanding of how to improve AUE genetically. In the context of increasing global food shortages and environmental pollution, our approach provides a potential means for enhancing NUE, with the real-life possibility of increasing crop yields without further increasing, indeed perhaps reducing, N fertilizer applications.

Materials and methods

Plant materials and growth conditions

Plant materials used in this work included wild-type (Col-0) Arabidopsis (*A. thaliana* L.) and the mutants *vtc1-1* (CS8326), *nramp1* (Gao et al. 2018), and *irt1-2* (Mao et al. 2014), derived from the Col-0 background. For overexpression of *VTC1* with green fluorescent protein (VTC1-GFP) in *vtc1-1*, the full coding sequence of *VTC1* was amplified by the polymerase chain reaction (PCR), using the SalI and BamHI sites, and cloned into pBinGFP4. The resulting plasmids were then introduced into *vtc1-1*, and the transgenic lines were confirmed by ammonium-sensitivity phenotypic recovery and GFP fluorescence intensity. Seeds were surface-sterilized and cold-treated at 4 °C for 48 h prior to being sown onto standard GM. The standard GM was as described previously (Li et al. 2013) and was composed of 2 mM KH_2PO_4, 5 mM $NaNO_3$, 2 mM $MgSO_4$, 1 mM $CaCl_2$, 50 μM H_3BO_3, 12 μM $MnSO_4$, 1 μM $ZnCl_2$, 1 μM $CuSO_4$, 0.2 μM Na_2MoO_4, 1% (w/v) sucrose, 0.8% (w/v) agar (Sinopharm Chemical Reagent Co., Ltd., 10000561) (pH 5.7, adjusted with 1 M NaOH); for treatment with Fe and/or NH_4^+, the GM medium was supplemented with the indicated concentrations of $(NH_4)_2SO_4$ and/or $FeSO_4$–EDTA (1:1). The day of sowing was considered day 0. Arabidopsis seedlings were grown, oriented vertically on the surface of the culture plates in a growth chamber, set to a 16 h light:8 h dark photoperiod, an irradiance of 100 μmol m^{-2} s^{-1}, and a temperature of 23 ± 1 °C. To study the effect of different iron forms, $FeSO_4$ or $FeCl_3$–EDTA (1:1) were added to the medium. For the dolomite (D) [$CaMg(CO_3)_2$, Macklin, C14535894] experiment, three dolomite (over a hundred-mesh sieve) application rates were used in the study: 0 (no addition of dolomite), 1 and 5 (application of dolomite at a rate of 1 and 5 g/L, respectively). The lettuce (*L. sativa*) variety used in our study was "Grand Rapids", and the Arabidopsis standard GM and the growth chamber conditions specified above were used for lettuce as well as for Arabidopsis. For treatment with NO_3^- and/or NH_4^+, the GM medium was supplemented with 5 mM $NaNO_3$ (−NH_4^+) and/or 2.5 mM $(NH_4)_2SO_4$ (+NH_4^+) plus 10, 100, or 200 μM $FeSO_4$–EDTA (1:1). Dolomite (5 g/L) was used for the dolomite experiment. The day of sowing was considered day 0.

Mineral content analysis

To measure NH_4^+ content, the roots were weighed and frozen in liquid nitrogen, and then extracted with 1 mL of 10 mM formic acid for the NH_4^+ content assay by high-performance liquid chromatography (HPLC), following derivatization with *o*-phthaldialdehyde, as described previously (Li et al. 2012). For the analysis of Fe and other ions, the roots were dried at 75 °C prior to analysis, and samples were digested with HNO_3 and subjected to Inductively Coupled Plasma Mass Spectrometry (ICP-MS, Agilent, Santa Clara, CA, USA).

Histochemical staining and GS activity analysis

The Fe-specific Perls staining was adapted from Roschzttardtz et al. (2009). Localization of Fe was observed and imaged using an Olympus BX51 microscope equipped with differential interference contrast (DIC) optics and an Olympus DP71 camera. VTC1-GFP expression in roots of *35S-VTC1-GFP* transgenic plants was observed using an LSM 710 confocal microscope (Zeiss), and the excitation (ex)/emission (em) parameters for confocal analyses were as follows: ex: 488 nm, em: 500 to 550 nm. GS activity was detected by a GS kit (BC0910, Solarbio) (Li et al. 2019). The specific enzyme activity (U/g FW) was defined as the amount of enzyme units catalyzing the transformation of 1 μM substrate per minute by the amount of fresh weight of seedlings in grams.

Measurement of net NH_4^+ fluxes with the noninvasive microtest technology system

The noninvasive microtest technology (NMT) technique (NMT system BIO-IM; Younger USA, LLC, Amherst, MA, USA) was used to monitor net NH_4^+ fluxes at the surface of the root tip transition zone. The NMT system and its use in detecting net NH_4^+ fluxes have been described in detail elsewhere (Li et al. 2010). The seedlings were grown on Fe^5−NH_4^+ medium for 7 d of growth and transferred to varying Fe and NH_4^+ treatments for 24 h. Then, the roots of Arabidopsis were equilibrated in the buffered measuring solution for 30 min. All measurements of net NH_4^+ fluxes were carried out at the Xuyue Science and Technology Co., Ltd (Beijing, China).

Measurement of 15N uptake rate

$^{15}NH_4^+$ and $^{15}NO_3^-$ uptake was measured as described previously (Tian et al. 2021). For $^{15}NH_4^+$ uptake, Arabidopsis seedlings were grown in GM plus 5 or 100 μM Fe medium for 10 d, then treated with 5 mM NH_4Cl concentration, identical to the following ^{15}N treatment, for 1 h before the uptake experiment. The seedlings were then treated with the indicated $^{15}NH_4Cl$ concentration for 30 min (pH 5.7). For $^{15}NO_3^-$ uptake, Arabidopsis seedlings were grown in GM with 5 mM NH_4^+ plus 5 or 100 μM Fe in the medium for 10 d, then treated with 5 mM $NaNO_3$ concentration, identical to the following ^{15}N treatment, for 1 h before the uptake experiment. The seedlings were then treated with the indicated $Na^{15}NO_3$ concentration for 30 min (pH 5.7). Atomic percent ^{15}N (50%) was detected using a Euro-EA Euro Vector elemental analyzer coupled with an IsoPrime mass spectrometer (GV Instruments). The total ^{15}N amount was calculated according to the equations by Drescher et al. (2020). Total N uptake (g) = %N in sample × DW (g)/100. The % atom ^{15}N in excess in sample = % atom ^{15}N in sample − 0.3663% (natural ^{15}N abundance). Total ^{15}N amount (g) = Total N uptake × (% atom ^{15}N in excess in sample/% atom ^{15}N in excess in fertilizer). The formula used for ^{15}N influx was: total ^{15}N amount/DW/0.5 h, yielding the amount of ^{15}N taken up per unit weight per unit time.

Root growth and seedling biomass measurements and assessment of NUE

The lengths of primary roots of individual Arabidopsis seedlings were measured directly with a ruler and using the ImageJ software, from digital images captured with a Canon G7 camera. Whole Arabidopsis and lettuce plants were sampled with 20 or 3 seedlings as a group, respectively, at 10 d after germination. All samples were kept in a dry oven at 80 °C for 3 d, and dry mass was measured. The total nitrogen and carbon contents were determined using a carbon/nitrogen elemental analyzer. For estimating NUE at the vegetative stage, the UI for N was calculated according to Wada et al. (2015) and represented as UI by division of the DW by the $N\%_{DW}$. For yield and NUE determination of lettuce, lettuce plants were grown on GM medium plus 5 mM $NaNO_3$ (−NH_4^+) and/or 2.5 mM $(NH_4)_2SO_4$ (+NH_4^+) for 30 d, and the yield was based on the fresh weight of shoots. NUE = Yield/supplied N.

Determination of rhizosphere pH in the agar rooting medium

The pH of the agar rooting medium was determined based on the method described by Zhu et al. (2019). The rooting medium was collected into a 15-mL centrifuge tube and then frozen at −20 °C overnight. The tube was thawed at room temperature to free the aqueous phase from the agar. The mixture was then filtered at room temperature and the pH of the supernatant was determined using a desktop pH electrode (Mettler Toledo). Measurements were taken on agar from four replicate plates per treatment, each of which contained 20 seedlings.

N-glycoprotein assays

The extent of mature N-glycoproteins of Arabidopsis roots after growth for 7 d was examined using anti-horseradish peroxidase (anti-HRP) (HRP, 1:200,000; Sigma–Aldrich), as described previously (Di et al. 2021). Intensities of the N-glycosylation zone were quantified using ImageJ software. The site-specific N-glycoproteomic assay and bioinformatic analysis was performed in Hangzhou Micron Biotechnology Co., Ltd. Briefly, samples of 7-d-old Arabidopsis root tissue were ground by liquid nitrogen into cell powder and then subjected to protein extraction. After trypsin digestion, peptide was desalted using a Strata X C18 SPE column (Phenomenex) and vacuum-dried. Then, after HPLC fractionation and affinity enrichment, the peptides were subjected to an NSI source followed by tandem mass spectrometry (MS/MS) in Orbitrap FusionTribrid (Thermo) coupled online to UPLC. The resulting MS/MS data were processed using the Maxquant search engine (v.1.5.2.8).

RNA isolation, reverse transcription-quantitative polymerase chain reaction (RT-qPCR), and sequencing

For RT-qPCR analysis, total RNA was extracted from Arabidopsis roots. Gene-specific primers for qPCR were designed using Primer-5 software (Supplementary Table S1), and the relative RNA abundance was normalized to the *ACTIN2* internal control ([mRNA]gene/[mRNA]*ACTIN2*). The RNA-seq assay was performed in Shanghai Biozeron Biotech. Co., Ltd. The methods for first-strand and double-stranded cDNA synthesis and purification, sample library construction, and differentially expressed gene (DEG) identification are as described in detail elsewhere (Di et al. 2021). Genes with a log_2-fold change > 0.5 and a P-value < 0.01 were considered differentially expressed (Lanver et al. 2018).

Statistical and graphical analyses

For all experiments, data were statistically analyzed using the SPSS 13.0 program (SPSS Chicago, IL, USA.). Details are shown in figure legends. Graphs were produced using GraphPad Prism 8.0.2.

Accession numbers

AtIRT1 (At4g19690), *AtNRAMP1* (At1g80830), *AtVTC1* (At2g39770), *AtLPR2* (At1g71040), *AtNUDX9* (At3g46200), *AtAHA9* (At1g80660), *AtPpi2* (At3g15340), and *AtACTIN2* (At3g18780).

Acknowledgments

We thank the Dr Chongwei Jin (Zhejiang University), Dr Chao-Feng Huang (Shanghai Center for Plant Stress Biology, Chinese Academy of Sciences), and ABRC of Ohio State University for sharing mutant seeds.

Author contributions

G.J.L. conceived the project and designed the experiments. G.J.L. carried out most of the experiments and analyzed the data. L.Z., J.L.W., and Z.Y.W. assisted in performing the experiments and analyzing the data. G.J.L., W.M.S., and H.J.K. wrote the manuscript. M.W. provided suggestions for the manuscript.

Supplementary data

The following materials are available in the online version of this article.

Supplementary Figure S1. Effects of Fe on seedling growth in Arabidopsis Col-0.

Supplementary Figure S2. Effect of Fe on GS activity and $C\%_{DW}$ in Arabidopsis.

Supplementary Figure S3. Effect of NH_4^+ and Fe on the mineral content.

Supplementary Figure S4. Effect of Fe on $^{15}NO_3^-$ and $^{15}NH_4^+$ uptake in Arabidopsis under elevated NH_4^+.

Supplementary Figure S5. Root Fe staining (Perls staining) in Col-0 and *vtc1-1* Fe^{100} + NH_4^+ medium.

Supplementary Figure S6. Effect of low Fe status on *NUDX9* gene expression in Col-0 and *vtc1-1* under elevated NH_4^+.

Supplementary Figure S7. Effect of high Fe on expression of VTC1-GFP in the absence of NH_4^+.

Supplementary Figure S8. Identification of representative compounds reducing NH_4^+ efflux in Arabidopsis.

Supplementary Figure S9. Effect of dolomite on $N\%_{DW}$ of Col-0.

Supplementary Figure S10. Effect of dolomite on DW of Col-0 in the absence of NH_4^+.

Supplementary Figure S11. Effects of $CaCO_3$ and $CaCl_2$ on DW of Col-0 under elevated NH_4^+.

Supplementary Figure S12. Effect of dolomite on pH and gene expression of *AHA9*, *Ppi2* under elevated NH_4^+.

Supplementary Figure S13. Mutation types of the *LPR2* gene in Col-0.

Supplementary Figure S14. Response of Arabidopsis *IRT1* and *NRAMP1* mutation to ammonium treatment.

Supplementary Table S1. Gene-specific primers used for RT-qPCR.

Supplementary Data Set 1. The differential distribution in N-glycosylation of proteins.

Supplementary Data Set 2. The DEGs between dolomite-treated and mock conditions under ammonium plus Fe^{100}.

Funding

This work was supported by the National Natural Science Foundation of China (no. 32372813; 32030099), the Taishan Scholars Program (no. tsqn202312287), the Youth Innovation Promotion Association CAS (no. 2020315), and the Chinese Academy of Sciences Innovation Program (ISSASIP2208).

Conflict of interest statement. None declared.

Data availability

The data that support the findings of this study are available in the article and in the Supporting Information of this article.

References

Anzi C, Pelucchi P, Vazzola V, Murgia I, Gomarasca S, Beretta Piccoli M, Morandini P. The proton pump interactor (Ppi) gene family of Arabidopsis thaliana: expression pattern of Ppi1 and characterisation of knockout mutants for Ppi1 and 2. Plant Biol. 2008:**10**(2):237–249. https://doi.org/10.1111/j.1438-8677.2007.00022.x

Balkos KD, Britto DT, Kronzucker HJ. Optimization of ammonium acquisition and metabolism by potassium in rice (*Oryza sativa* L. cv.

IR-72). Plant Cell Environ. 2010:**33**(1):23–34. https://doi.org/10.1111/j.1365-3040.2009.02046.x

Bao A, Liang Z, Zhao Z, Cai H. Overexpressing of *OsAMT1-3*, a high affinity ammonium transporter gene, modifies rice growth and carbon-nitrogen metabolic status. Int J Mol Sci. 2015:**16**(5):9037–9063. https://doi.org/10.3390/ijms16059037

Barth C, Gouzd ZA, Steele HP, Imperio RM. A mutation in GDP-mannose pyrophosphorylase causes conditional hypersensitivity to ammonium, resulting in *Arabidopsis* root growth inhibition, altered ammonium metabolism, and hormone homeostasis. J Exp Bot. 2010:**61**(2):379–394. https://doi.org/10.1093/jxb/erp310

Brauer EK, Shelp BJ. Nitrogen use efficiency: re-consideration of the bioengineering approach. Botany. 2010:**88**(2):103–109. https://doi.org/10.1139/B09-111

Britto DT, Balkos KD, Becker A, Coskun D, Huynh WQ, Kronzucker HJ. Potassium and nitrogen poising: physiological changes and biomass gains in rice and barley. Can J Plant Sci. 2014:**94**(6):1085–1089. https://doi.org/10.4141/cjps2013-143

Britto DT, Kronzucker HJ. NH_4^+ toxicity in higher plants: a critical review. J Plant Physiol. 2002:**159**(6):567–584. https://doi.org/10.1078/0176-1617-0774

Britto DT, Kronzucker HJ. Nitrogen acquisition, PEP carboxylase, and cellular pH homeostasis: new views on old paradigms. Plant Cell Environ. 2005:**28**(11):1396–1409. https://doi.org/10.1111/j.1365-3040.2005.01372.x

Britto DT, Siddiqi MY, Glass A, Kronzucker HJ. Futile transmembrane NH_4^+ cycling: a cellular hypothesis to explain ammonium toxicity in plants. Proc Natl Acad Sci U S A. 2001:**98**(7):4255–4258. https://doi.org/10.1073/pnas.061034698

Castaings L, Caquot A, Loubet S, Curie C. The high-affinity metal transporters NRAMP1 and IRT1 team up to take up iron under sufficient metal provision. Sci Rep. 2016:**6**:37222. https://doi.org/10.1038/srep37222

Chen G, Guo SW, Kronzucker HJ, Shi WM. Nitrogen use efficiency (NUE) in rice links to NH_4^+ toxicity and futile NH_4^+ cycling in roots. Plant Soil. 2013:**369**(1–2):351–363. https://doi.org/10.1007/s11104-012-1575-y

Chen KE, Chen HY, Tseng CS, Tsay YF. Improving nitrogen use efficiency by manipulating nitrate remobilization in plants. Nat Plants. 2020a:**6**(9):1126–1135. https://doi.org/10.1038/s41477-020-00758-0

Chen M, Chen G, Di D, Kronzucker HJ, Shi W. Higher nitrogen use efficiency (NUE) in hybrid "super rice" links to improved morphological and physiological traits in seedling roots. J Plant Physiol. 2020b:**251**:153191. https://doi.org/10.1016/j.jplph.2020.153191

Coleto I, Bejarano I, Marín-Peña AJ, Medina J, Rioja C, Burow M, Marino D. *Arabidopsis thaliana* transcription factors *MYB28* and *MYB29* shape ammonium stress responses by regulating Fe homeostasis. New Phytol. 2021:**229**(2):1021–1035. https://doi.org/10.1111/nph.16918

Coleto I, Marín-Peña AJ, Urbano-Gámez JA, González-Hernández AI, Shi W, Li G, Marino D. Interaction of ammonium nutrition with essential mineral cations. J Exp Bot. 2023:**74**(19):6131–6144. https://doi.org/10.1093/jxb/erad215

Coskun D, Britto DT, Kronzucker HJ. The nitrogen-potassium intersection: membranes, metabolism, and mechanism. Plant Cell Environ. 2017a:**40**(10):2029–2041. https://doi.org/10.1111/pce.12671

Coskun D, Britto DT, Shi WM, Kronzucker HJ. How plant root exudates shape the nitrogen cycle. Trends Plant Sci. 2017b:**22**(8):661–673. https://doi.org/10.1016/j.tplants.2017.05.004

Di DW, Sun L, Wang M, Wu JJ, Kronzucker HJ, Fang S, Chu JF, Shi WM, Li GJ. WRKY46 promotes ammonium tolerance in *Arabidopsis* by repressing NUDX9 and indole-3-acetic acid-conjugating genes and by inhibiting ammonium efflux in the root elongation zone. New Phytol. 2021:**232**(1):190–207. https://doi.org/10.1111/nph.17554

Drescher GL, Da Silva LS, Sarfaraz Q, Roberts TL, Nicoloso FT, Schwalbert R, Ramos Marques AC. Available nitrogen in paddy soils depth: influence on rice root morphology and plant nutrition. J Soil Sci Plant Nutr. 2020:**20**(3):1029–1041. https://doi.org/10.1007/s42729-020-00190-5

Esteban R, Ariz I, Cruz C, Moran JF. Review: mechanisms of ammonium toxicity and the quest for tolerance. Plant Sci. 2016:**248**:92–101. https://doi.org/10.1016/j.plantsci.2016.04.008

Fan XR, Tang Z, Tan YW, Xu GH. Overexpression of a pH-sensitive nitrate transporter in rice increases crop yields. Proc Natl Acad Sci U S A. 2016:**113**(26):7118–7123. https://doi.org/10.1073/pnas.1525184113

Gao HL, Xie WX, Yang CH, Xu JY, Li JJ, Wang H, Chen X, Huang CF. NRAMP2, a trans-Golgi network-localized manganese transporter, is required for *Arabidopsis* root growth under manganese deficiency. New Phytol. 2018:**217**(1):179–193. https://doi.org/10.1111/nph.14783

Good AG, Shrawat AK, Muench DG. Can less yield more? Is reducing nutrient input into the environment compatible with maintaining crop production? Trends Plant Sci. 2004:**9**(12):597–605. https://doi.org/10.1016/j.tplants.2004.10.008

Green LS, Rogers EE. FRD3 controls iron localization in Arabidopsis. Plant Physiol. 2004:**136**(1):2523–2531. https://doi.org/10.1104/pp.104.045633

Hachiya T, Inaba J, Wakazaki M, Sato M, Toyooka K, Miyagi A, Kawai-Yamada M, Sugiura D, Nakagawa T, Kiba T, et al. Excessive ammonium assimilation by plastidic glutamine synthetase causes ammonium toxicity in *Arabidopsis thaliana*. Nat Commun. 2021:**12**(1):4944. https://doi.org/10.1038/s41467-021-25238-7

Hachiya T, Sakakibara H. Interactions between nitrate and ammonium in their uptake, allocation, assimilation, and signaling in plants. J Exp Bot. 2017:**68**:2501–2512. https://doi.org/10.1093/jxb/erw449

Hachiya T, Terashima I, Noguchi K. Increase in respiratory cost at high growth temperature is attributed to high protein turnover cost in *Petunia* x *hybrida* petals. Plant Cell Environ. 2007:**30**(10):1269–1283. https://doi.org/10.1111/j.1365-3040.2007.01701.x

Hoque MS, Masle J, Udvardi MK, Ryan PR, Upadhyaya NM. Over-expression of the rice *OsAMT1-1* gene increases ammonium uptake and content, but impairs growth and development of plants under high ammonium nutrition. Funct Plant Biol. 2006:**33**(2):153–163. https://doi.org/10.1071/FP05165

Hu B, Wang W, Ou SJ, Tang JY, Li H, Che RH, Zhang ZH, Chai XY, Wang HR, Wang YQ, et al. Variation in *NRT1.1B* contributes to nitrate-use divergence between rice subspecies. Nat Genetics. 2015:**47**(7):834–838. https://doi.org/10.1038/ng.3337

Huang XZ, Qian Q, Liu ZB, Sun HY, He SY, Luo D, Xia GM, Chu CC, Li JY, Fu XD. Natural variation at the *DEP1* locus enhances grain yield in rice. Nat Genetics. 2009:**41**(4):494–497. https://doi.org/10.1038/ng.352

Kempinski CF, Haffar R, Barth C. Toward the mechanism of NH_4^+ sensitivity mediated by *Arabidopsis* GDP-mannose pyrophosphorylase. Plant Cell Environ. 2011:**34**(5):847–858. https://doi.org/10.1111/j.1365-3040.2011.02290.x

Kronzucker HJ, Britto DT, Davenport RJ, Tester M. Ammonium toxicity and the real cost of transport. Trends Plant Sci. 2001:**6**(8):335–337. https://doi.org/10.1016/S1360-1385(01)02022-2

Kronzucker HJ, Siddiqi MY, Glass ADM. Conifer root discrimination against soil nitrate and the ecology of forest succession. Nature. 1997:**385**(6611):59–61. https://doi.org/10.1038/385059a0

Kronzucker HJ, Siddiqi MY, Glass ADM, Britto DT. Root ammonium transport efficiency as a determinant in forest colonization patterns: an hypothesis. Physiol Plant. 2003:**117**(2):164–170. https://doi.org/10.1034/j.1399-3054.2003.00032.x

Kronzucker HJ, Siddiqi MY, Glass ADM, Kirk GJD. Nitrate-ammonium synergism in rice: a subcellular analysis. Plant Physiol. 1999:**119**(3):1041–1046. https://doi.org/10.1104/pp.119.3.1041

Kronzucker HJ, Siddiqi MY, Glass ADM, Kirk GJD. Comparative kinetic analysis of ammonium and nitrate acquisition by tropical lowland rice: implications for rice cultivation and yield potential. New Phytol. 2000:**145**(3):471–476. https://doi.org/10.1046/j.1469-8137.2000.00606.x

Lanver D, Müller AN, Happel P, Schweizer G, Haas FB, Franitza M, Pellegrin C, Reissmann S, Altmüller J, Rensing SA, et al. The biotrophic development of *Ustilago maydis* studied by RNA-seq analysis. Plant Cell. 2018:**30**(2):300–323. https://doi.org/10.1105/tpc.17.00764

Li BH, Li GJ, Kronzucker HJ, Baluška F, Shi WM. Ammonium stress in *Arabidopsis*: signaling, genetic loci, and physiological targets. Trends Plant Sci. 2014:**19**(2):107–114. https://doi.org/10.1016/j.tplants.2013.09.004

Li GJ, Dong GQ, Li BH, Li Q, Kronzucker HJ, Shi WM. Isolation and characterization of a novel ammonium overly sensitive mutant, *amos2*, in *Arabidopsis thaliana*. Planta. 2012:**235**(2):239–252. https://doi.org/10.1007/s00425-011-1504-y

Li GJ, Li BH, Dong GQ, Feng XY, Kronzucker HJ, Shi WM. Ammonium-induced shoot ethylene production is associated with the inhibition of lateral root formation in *Arabidopsis*. J Exp Bot. 2013:**64**(5):1413–1425. https://doi.org/10.1093/jxb/ert019

Li GJ, Zhang L, Wang M, Di DW, Kronzucker HJ, Shi WM. The Arabidopsis *AMOT1/EIN3* gene plays an important role in the amelioration of ammonium toxicity. J Exp Bot. 2019:**70**(4):1375–1388. https://doi.org/10.1093/jxb/ery457

Li GJ, Zhang L, Wu JL, Yue XW, Wang M, Sun L, Di DW, Kronzucker HJ, Shi WM. OsEIL1 protects rice growth under NH_4^+ nutrition by regulating OsVTC1-3-dependent N-glycosylation and root NH_4^+ efflux. Plant Cell Environ. 2022:**45**(5):1537–1553. https://doi.org/10.1111/pce.14283

Li Q, Li BH, Kronzucker HJ, Shi WM. Root growth inhibition by NH_4^+ in *Arabidopsis* is mediated by the root tip and is linked to NH_4^+ efflux and GMPase activity. Plant Cell Environ. 2010:**33**(9):1529–1542. https://doi.org/10.1111/j.1365-3040.2010.02162.x

Liu KX, Sakuraba Y, Ohtsuki N, Yang ML, Ueda Y, Yanagisawa S. CRISPR/Cas9-mediated elimination of OsHHO3, a transcriptional repressor of three *AMMONIUM TRANSPORTER1* genes, improves nitrogen use efficiency in rice. Plant Biotechnol J. 2023a:**21**(11):2169–2172. https://doi.org/10.1111/pbi.14167

Liu XX, Zhang HH, Zhu QY, Ye JY, Zhu YX, Jing XT, Du WX, Zhou M, Lin XY, Zheng SJ, et al. Phloem iron remodels root development in response to ammonium as the major nitrogen source. Nat Commun. 2022a:**13**(1):561. https://doi.org/10.1038/s41467-022-28261-4

Liu XX, Zhu XF, Xue DW, Zheng SJ, Jin CW. Beyond iron-storage pool: functions of plant apoplastic iron during stress. Trends Plant Sci. 2023b:**28**(8):941–954. https://doi.org/10.1016/j.tplants.2023.03.007

Liu Y, Maniero RA, Giehl RFH, Melzer M, Steensma P, Krouk G, Fitzpatrick TB, von Wirén N. PDX1.1-dependent biosynthesis of vitamin B6 protects roots from ammonium-induced oxidative stress. Mol Plant. 2022b:**15**(5):820–839. https://doi.org/10.1016/j.molp.2022.01.012

Liu Y, Xu GH. Nitrogen-iron interaction as an emerging factor to impact crop productivity and nutrient use efficiency. Mol Plant. 2023:**16**(11):1727–1729. https://doi.org/10.1016/j.molp.2023.10.002

Liu YQ, Wang HR, Jiang ZM, Wang W, Xu RN, Wang QH, Zhang ZH, Li AF, Liang Y, Ou SJ, et al. Genomic basis of geographical adaptation to soil nitrogen in rice. Nature. 2021:**590**(7847):600–605. https://doi.org/10.1038/s41586-020-03091-w

Ma XL, Zhu CH, Yang N, Gan LJ, Xia K. γ-Aminobutyric acid addition alleviates ammonium toxicity by limiting ammonium accumulation in rice (*Oryza sativa*) seedlings. Physiol Plant. 2016:**158**(4):389–401. https://doi.org/10.1111/ppl.12473

Mao QQ, Guan MY, Lu KX, Du ST, Fan SK, Ye Y, Lin XY, Jin CW. Inhibition of nitrate transporter 1.1-controlled nitrate uptake reduces cadmium uptake in Arabidopsis. Plant Physiol. 2014:**166**(2):934–944. https://doi.org/10.1104/pp.114.243766

Meier M, Liu Y, Lay-Pruitt KS, Takahashi H, von Wirén N. Auxin-mediated root branching is determined by the form of available nitrogen. Nat Plants. 2020:**6**(9):1136–1145. https://doi.org/10.1038/s41477-020-00756-2

Min J, Sun HJ, Wang Y, Pan Y, Kronzucker HJ, Zhao D, Shi WM. Mechanical side-deep fertilization mitigates ammonia volatilization and nitrogen runoff and increases profitability in rice production independent of fertilizer type and split ratio. J Clean Prod. 2021:**316**:128370. https://doi.org/10.1016/j.jclepro.2021.128370

Ohkubo Y, Tanaka M, Tabata R, Ogawa-Ohnishi M, Matsubayashi Y. Shoot-to-root mobile polypeptides involved in systemic regulation of nitrogen acquisition. Nat Plants. 2017:**3**(4):17029. https://doi.org/10.1038/nplants.2017.29

Palmgren MG. PLANT PLASMA MEMBRANE H^+-ATPases: powerhouses for nutrient uptake. Annu Rev Plant Biol. 2001:**52**(1):817–845. https://doi.org/10.1146/annurev.arplant.52.1.817

Qin C, Qian WQ, Wang WF, Wu Y, Yu CM, Jiang XH, Wang DW, Wu P. GDP-mannose pyrophosphorylase is a genetic determinant of ammonium sensitivity in *Arabidopsis thaliana*. Proc Natl Acad Sci U S A. 2008:**105**(47):18308–18313. https://doi.org/10.1073/pnas.0806168105

Roosta HR, Schjoerring JK. Effects of ammonium toxicity on nitrogen metabolism and elemental profile of cucumber plants. J Plant Nut. 2007:**30**(11):1933–1951. https://doi.org/10.1080/01904160701629211

Roosta HR, Schjoerring JK. Root carbon enrichment alleviates ammonium toxicity in cucumber plants. J Plant Nutr. 2008:**31**(5):941–958. https://doi.org/10.1080/01904160802043270

Roschzttardtz H, Conéjéro G, Curie C, Mari S. Identification of the endodermal vacuole as the iron storage compartment in the *Arabidopsis* embryo. Plant Physiol. 2009:**151**(3):1329–1338. https://doi.org/10.1104/pp.109.144444

Rubio-Asensio JS, Bloom AJ. Inorganic nitrogen form: a major player in wheat and Arabidopsis responses to elevated CO_2. J Exp Bot. 2017:**68**(10):2611–2625. https://doi.org/10.1093/jxb/erw465

Song Y, Wan GY, Wang JX, Zhang ZS, Xia JQ, Sun LQ, Lu J, Ma CX, Yu LH, Xiang CB, et al. Balanced nitrogen-iron sufficiency boosts grain yield and nitrogen use efficiency by promoting tillering. Mol Plant. 2023:**16**(10):1661–1677. https://doi.org/10.1101/2023.02.28.530550

Strasser R, Altmann F, Mach L, Glössl J, Steinkellner H. Generation of *Arabidopsis thaliana* plants with complex *N*-glycans lacking β1,2-linked xylose and core α1,3-linked fucose. FEBS Lett. 2004:**561**(1–3):132–136. https://doi.org/10.1016/S0014-5793(04)00150-4

Subbarao GV, Searchinger TD. Opinion: A "more ammonium solution" to mitigate nitrogen pollution and boost crop yields. Proc Natl Acad Sci U S A. 2021:**118**(22):e2107576118. https://doi.org/10.1073/pnas.2107576118

Sun HJ, Zhang HL, Powlson D, Min J, Shi WM. Rice production, nitrous oxide emission and ammonia volatilization as impacted by the nitrification inhibitor 2-chloro-6-(trichloromethyl)-pyridine. Field Crop Res. 2015:**173**:1–7. https://doi.org/10.1016/j.fcr.2014.12.012

Suriyagoda LDB, Sirisena DN, Somaweera KATN, Dissanayake A, De Costa WAJM, Lambers H. Incorporation of dolomite reduces iron toxicity, enhances growth and yield, and improves phosphorus and potassium nutrition in lowland rice (*Oryza sativa* L). Plant Soil. 2017:**410**(1–2):299–312. https://doi.org/10.1007/s11104-016-3012-0

Szczerba MW, Britto DT, Balkos KD, Kronzucker HJ. Alleviation of rapid, futile ammonium cycling at the plasma membrane by potassium reveals K^+-sensitive and -insensitive components of NH_4^+ transport. J Exp Bot. 2008:**59**(2):303–313. https://doi.org/10.1093/jxb/erm309

Tanaka H, Maruta T, Ogawa T, Tanabe N, Tamoi M, Yoshimura K, Shigeoka S. Identification and characterization of *Arabidopsis* AtNUDX9 as a GDP-d-mannose pyrophosphohydrolase: its involvement in root growth inhibition in response to ammonium. J Exp Bot. 2015:**66**(19):5797–5808. https://doi.org/10.1093/jxb/erv281

Tian WH, Ye JY, Cui MQ, Chang JB, Liu Y, Li GX, Wu YR, Xu JM, Harberd NP, Mao CZ, et al. A transcription factor STOP1-centered pathway coordinates ammonium and phosphate acquisition in *Arabidopsis*. Mol Plant. 2021:**14**(9):1554–1568. https://doi.org/10.1016/j.molp.2021.06.024

Tsay YF, Schroeder JI, Feldmann KA, Crawford NM. The herbicide sensitivity gene *CHL1* of *Arabidopsis* encodes a nitrate-inducible nitrate transporter. Cell. 1993:**72**(5):705–713. https://doi.org/10.1016/0092-8674(93)90399-B

Vert G, Grotz N, Dédaldéchamp F, Gaymard F, Guerinot ML, Briat J-F, Curie C. IRT1, an Arabidopsis transporter essential for iron uptake from the soil and for plant growth. Plant Cell. 2002:**14**(6): 1223–1233. https://doi.org/10.1105/tpc.001388

Vidal EA, Alvarez JM, Araus V, Riveras E, Brooks MD, Krouk G, Ruffel S, Lejay L, Crawford NM, Coruzzi GM, et al. Nitrate in 2020: thirty years from transport to signaling networks. Plant Cell. 2020:**32**(7):2094–2119. https://doi.org/10.1105/tpc.19.00748

Wada S, Hayashida Y, Izumi M, Kurusu T, Hanamata S, Kanno K, Kojima S, Yamaya T, Kuchitsu K, Makino A, et al. Autophagy supports biomass production and nitrogen use efficiency at the vegetative stage in rice. Plant Physiol. 2015:**168**(1):60–73. https://doi.org/10.1104/pp.15.00242

Wu K, Wang SS, Song WZ, Zhang JQ, Wang Y, Liu Q, Yu JP, Ye YF, Li S, Chen JF, et al. Enhanced sustainable green revolution yield via nitrogen-responsive chromatin modulation in rice. Science. 2020:**367**(6478):641. https://doi.org/10.1126/science.aaz2046

Xiao CB, Sun DD, Liu BB, Fang XM, Li PC, Jiang Y, He MM, Li J, Luan S, He K. Nitrate transporter NRT1.1 and anion channel SLAH3 form a functional unit to regulate nitrate-dependent alleviation of ammonium toxicity. J Integr Plant Biol. 2022:**64**(4):942–957. https://doi.org/10.1111/jipb.13239

Xie YM, Lv YD, Jia LT, Zheng LL, Li YH, Zhu M, Tian MJ, Wang M, Qi WC, Luo L, et al. Plastid-localized amino acid metabolism coordinates rice ammonium tolerance and nitrogen use efficiency. Nat Plant. 2023:**9**(9):1514–1529. https://doi.org/10.1038/s41477-023-01494-x

Xu ZR, Cai ML, Yang Y, You TT, Ma JF, Wang P, Zhao FJ. The ferroxidases LPR1 and LPR2 control iron translocation in the xylem of *Arabidopsis* plants. Mol Plant. 2022:**15**(12):1962–1975. https://doi.org/10.1016/j.molp.2022.11.003

Xu GH, Fan XR, Miller AJ. Plant nitrogen assimilation and use efficiency. Ann Rev Plant Biol. 2012:**63**(1):153–182. https://doi.org/10.1146/annurev-arplant-042811-105532

Zhang L, Song HY, Li BH, Wang M, Di DW, Lin XY, Kronzucker HJ, Shi WM, Li GJ. Induction of S-nitrosoglutathione reductase protects root growth from ammonium toxicity by regulating potassium homeostasis in Arabidopsis and rice. J Exp Bot. 2021:**72**(12):4548–4564. https://doi.org/10.1093/jxb/erab140

Zhang M, Ding M, Xu F, Afzal MR, Chen X, Zeng H, Yan F, Zhu Y. Involvement of plasma membrane H^+-ATPase in the ammonium-nutrition response of barley roots. J Plant Nutr Soil Sci. 2018:**181**(6): 878–885. https://doi.org/10.1002/jpln.201800045

Zhu J, Fang XZ, Dai YJ, Zhu YX, Chen HS, Lin XY, Jin CW. Nitrate transporter 1.1 alleviates lead toxicity in *Arabidopsis* by preventing rhizosphere acidification. J Exp Bot. 2019:**70**(21):6363–6374. https://doi.org/10.1093/jxb/erz374

Zhu QY, Wang Y, Liu XX, Ye JY, Zhou M, Jing XT, Du WX, Hu WJ, He C, Zhu YX, et al. The ferroxidases are critical for Fe(II) oxidation in xylem to ensure a healthy Fe allocation in *Arabidopsis thaliana*. Front Plant Sci. 2022:**13**:958984. https://doi.org/10.3389/fpls.2022.958984

Zhu Y, Di T, Xu G, Chen X, Zeng H, Yan F, Shen Q. Adaptation of plasma membrane H^+-ATPase of rice roots to low pH as related to ammonium nutrition. Plant Cell Environ. 2009:**32**(10):1428–1440. https://doi.org/10.1111/j.1365-3040.2009.02009.x